Elsevier Editorial System(tm) for Engineering Analysis with Boundary Elements
Manuscript Draft

Manuscript Number: EABE-D-14-00245R1

Title: Boundary Element Analysis of Stiffened Panels with Repair Patches

Article Type: Full Length Article

Keywords: Repair patches; Reissner plate; Assembled plate structures; Rivets; Adhesive bonding; Dual boundary element method

Corresponding Author: Professor Ferri Aliabadi,

Corresponding Author's Institution: Imperial College

First Author: Ferri Aliabadi

Order of Authors: Ferri Aliabadi

Abstract: In this paper a boundary element method for analysis of fractured stiffened panels repaired with riveted or adhesively bonded patches is presented. In order to achieve such a formulation, several boundary element formulations involving the membrane and bending of displacement, and, stress resultants are coupled together to analyse the model. The multi-region formulation is used to simulate the stiffeners, which are modelled as an assembly. They are then connected to the sheets to form the stiffened panels by means of a rivet formulation. The dual boundary element method is used to simulate the presence of cracks, and the patches, treated as independent plates, are joined to the panel either with rivets or adhesive. A boundary element formulation for adhesive bonding is implemented to model the adhesively bonded patches. The Crack Opening Displacements (COD) method and the J-integral are implemented to evalute the required fracture parameters. Examples presented include a wing box with a three spar section, with fully stiffened skin, and, the skin is considered to have a crack and a repair patch is used on top of the crack to stop its growth.

Response to Reviewers: Thank you for highlighting the missing references and figures numbers as well as certain typo’s. We have corrected all the highlighted items.

Detailed Response to Reviewers

Thank you for highlighting the missing references and figures numbers as well as certain typo's. We have corrected all the highlighted items.

Boundary Element Analysis of Stiffened Panels with Repair Patches

C.Di Pisa[1], M.H. Aliabadi[2]
[1]Department of Engineering, Queen Mary, University of London, London E1 4NS, UK
[2]Department of Aeronautics, Imperial College, London SW7 2BY, UK

Abstract

In this paper a boundary element method for analysis of fractured stiffened panels repaired with riveted or adhesively bonded patches is presented. In order to achieve such a formulation, several boundary element formulations involving the membrane and bending of displacement, and, stress resultants are coupled together to analyse the model. The multi-region formulation is used to simulate the stiffeners, which are modelled as an assembly. They are then connected to the sheets to form the stiffened panels by means of a rivet formulation. The dual boundary element method is used to simulate the presence of cracks, and the patches, treated as independent plates, are joined to the panel either with rivets or adhesive. A boundary element formulation for adhesive bonding is implemented to model the adhesively bonded patches. The Crack Opening Displacements (COD) method and the J-integral are implemented to evalute the required fracture parameters. Examples presented include a wing box with a three spar section, with fully stiffened skin, and, the skin is considered to have a crack and a repair patch is used on top of the crack to stop its growth.

Keywords: Repair patches; Boundary Elements; Reissner plate; Assembled plate structures; Rivets; Adhesive bonding; Dual boundary element method

Introduction

In the aeronautical industry, repairs are largely employed to restore the strength and to improve fatigue life of damage stiffened panels. They consist on applying an extra panel (patch), either riveted or bonded with adhesive, on top of the damage. Numerical modelling of repairs is a feature which is intensively sought in computational mechanics. The Finite Element Method (FEM) present, to date, the only numerical method capable of modelling such complex problems[1, 8, 35, 49, 36, 57].

The boundary element method has enjoyed some success in analysing relatively large scale industrial applications, although mostly limited to two and three-dimensional problems. The application of the boundary element method to the classical plate theory was first proposed by Jaswon, Maiti and Symm[28]. Later, the development of the direct formulation based on the Kirchhoff theory[33] was introduced by Forbes and Robinson[22], followed by Bezine[12], Stern[59] and Tottenham[65]. Hartmann and Zomantel[25], further developed the method, and implemented it for plate with relatively complex geometries and loadings. Following the above work, others (Tanaka and Miyazaki[62], Fernandes and Venturini[68], Paiva and Aliabadi[42], Albuquerque[2] among others[31, 32, 55, 3, 9, 41, 58, 60, 23, 29, 34, 64, 72]) have further extended the formulation for the classical plate.

Application of the direct BEM for the analysis of Reissner plate [24, 50] was presented by Vander Ween[67]. Later, Karam and Telles[30] extended the formulation to infinite regions. Barcellos and Silva[10] presented a similar formulation to that of [67]for the Mindlin plate model. Their formulation differed by the shear factor constant. Later, Westphal and Barcellos[72] investigated the importance of the neglected terms in the fundamental solutions derived in [67]. For thin-walled structures recent advances have shown BEM to be capable of modelling cracks in linear and nonlinear (geometric and material behavior) regimes. Industrial problems such as those in the aeronautics industry require a model to include thin-walls (aircraft skin) with stiffeners of different shape and patches in the form of a tear strap or repair patches to be ether riveted or adhesively

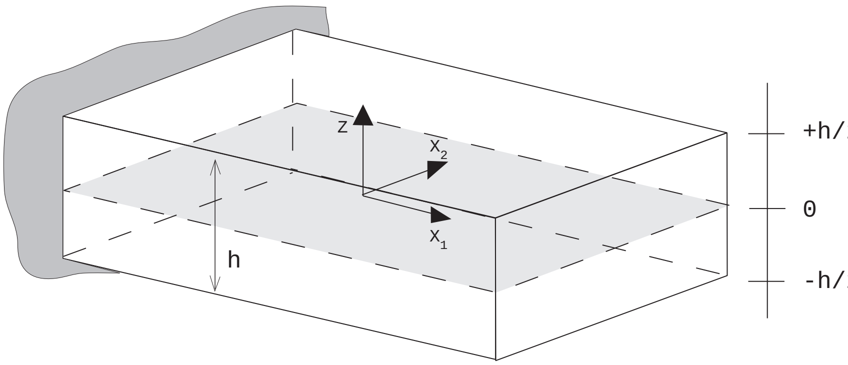

Figure 1: Single plate geometry

bonded. The interest lies in the interaction of these assembled features and behavior and growth of a crack in the skin in presence of these features. BEM formulations, often include one feature at a time as including all the features and their interactions, although assumed to be possible pose difficulties in implementation. In this paper, a feasibility study of applying the Boundary Element Method (BEM) to the analysis of these problems is presented. Previous works on stiffened plates and shells can be found in [74] for BEM where the stiffeners are modelled as beams. Cracks are modelled using the Dual Boundary Element Method (DBEM), as proposed by in [13, 14, 19]. Several works on cracks modelling with BEM can be found; reviews can be found in [5], [6] and [21]. The stiffeners can be attached to the sheets with rivets. BEM formulation for two-dimensional riveted panels with cracks can be found in [52], while applications to riveted repairs in [54] and [70]. Widagdoo and Aliabadi in [75] analyzed the effect of different materials for composite riveted patches. The patches are added using rivets and adhesive bonding. A BEM formulation has been proposed by Young et al. [69], using domain cells to evaluate the domain integrals; Salgado and Aliabadi [53] implemented the DRM in order to transfer to the boundary these integrals. Here, a BEM formulation combining all the previous features is presented and is applied to the study a complex stiffened structure. Recent advances in BEM [4, 11, 26, 56] and its application to plate can be found in [15, 7, 46, 45, 66, 27, 63, 73, 44, 16, 37].

In this paper, the above formulations are extended to allow for modelling of complex structures including all the features of stiffeners and repair patches. The stiffeners can be modelled as intact or broken are formulated as an assembled structure using a multi-domain formulation. The repair patches can be either riveted or adhesively bonded. Several examples are presented to demonstrate the applicability of the above formulation.

Multi-region boundary element formulation for assembled plate structures

Following Aliabadi [4], by means of Betti's theorem, it is possible to write the boundary displacement integral equations for the plate in figure (1) as follows:

$$C^{m}_{\alpha\beta}(\mathbf{x}')u_\beta(\mathbf{x}') + -\!\!\!\!\!\!\int T(\mathbf{x}',\mathbf{x})u_\beta(\mathbf{x})d\Gamma - \int_\Gamma U_{\alpha\beta}(\mathbf{x}',\mathbf{x})t_\beta(\mathbf{x})d\Gamma = \int_\Omega U_{\alpha\beta}(\mathbf{x}',\mathbf{X})f_\beta(\mathbf{X})d\Omega \tag{1}$$

$$C^{b}_{ik}(\mathbf{x}')w_k(\mathbf{x}') + -\!\!\!\!\!\!\int P_{ik}(\mathbf{x}',\mathbf{x})w_k(\mathbf{x})d\Gamma - \int_\Gamma W_{ik}(\mathbf{x}',\mathbf{x})p_k(\mathbf{x})d\Gamma = \int_\Omega W_{ik}(\mathbf{x}',\mathbf{X})q_k(\mathbf{X})d\Omega \tag{2}$$

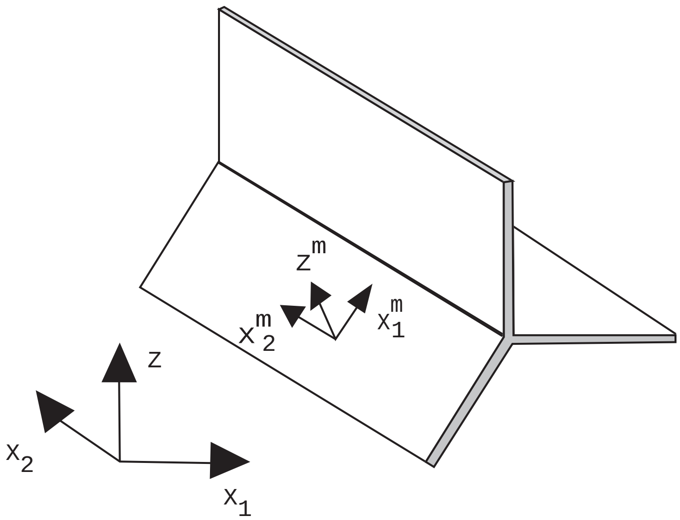

Figure 2: Generic assembled plate

where $u_\beta(\mathbf{x}')$ and $w_k(\mathbf{x}')$ are displacements and rotation at source point $\mathbf{x}' \in \Gamma$; $u_\beta(\mathbf{x})$, $w_k(\mathbf{x})$, $t_\beta(\mathbf{x})$ and $p_k(\mathbf{x})$ are displacements, rotations, moments and tractions at field point $\mathbf{x} \in \Gamma$; $f_\beta(\mathbf{X})$ and $q_k(\mathbf{X})$ are domain loads at field point $\mathbf{X} \in \Omega$; $T_{\alpha\beta}$, $U_{\alpha\beta}$, P_{ik} and W_{ik} are the fundamental solutions and they have been found by Kelvin for the membrane problem ($T_{\alpha\beta}$, $U_{\alpha\beta}$) and by Vander Weeën [67] for the bending problem ($P_{\alpha\beta}$, $W_{\alpha\beta}$). The symbol $⨍$ denotes Cauchy principal value integral, coefficients $C^m_{\alpha\beta}(\mathbf{x}')$, $C^b_{ik}(\mathbf{x}')$ are functions of the geometry at the boundary point and can be determined by rigid body movements as shown in [4, 48].The domain integrals in equations (1) and (2) are transferred to the boundary by means of the Dual Reciprocity Method (DRM) as described in [4]. For a collocation point within the domain of the plate (DRM collocation point), the displacement integral equations can be written as follows:

$$u_\beta(\mathbf{X}') + \int_\Gamma T_{\alpha\beta}(\mathbf{X}', \mathbf{x}) u_\beta(\mathbf{x}) d\Gamma = \int_\Gamma U_{\alpha\beta}(\mathbf{X}', \mathbf{x}) t_\beta(\mathbf{x}) d\Gamma + \int_\Omega U_{\alpha\beta}(\mathbf{X}', \mathbf{X}) f_\beta(\mathbf{X}) d\Omega \tag{3}$$

$$w_k(\mathbf{X}') + \int_\Gamma P_{ik}(\mathbf{X}', \mathbf{x}) w_k(\mathbf{x}) d\Gamma = \int_\Gamma W_{ik}(\mathbf{X}', \mathbf{x}) p_k(\mathbf{x}) d\Gamma + \int_\Omega W_{ik}(\mathbf{X}', \mathbf{X}) q_k(\mathbf{X}) d\Omega \tag{4}$$

where the collocation point $\mathbf{X}' \in \Omega$. Fundamental solutions are the same as for equations (1) and (2).

In order to model assembled plate structures, a multi-region formulation is implemented similarly as that proposed by Dirgantara in ([17]). Consider M plates joined along a common edge (figure (2)). For each plate it is possible to write the boundary integral equation independently, in local coordinates x_i^m, where $i = 1, 2, 3$ and $m = 1, .., M$. Then compatibility equations for displacements and equilibrium equations along the joining line can be enforced. Different cases have to be considered, according to the geometry.

In the simple case of two plates with same axis orientation, joined along a generic line with eccentricity e, the equations expressing continuity of displacements and equilibrium of stresses across the join can be written as follows:

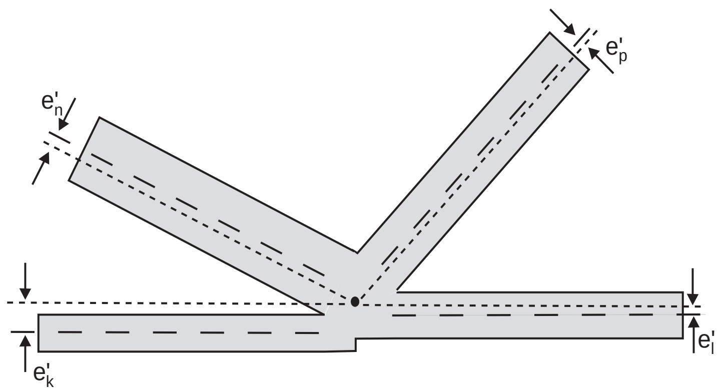

Figure 3: Angled plates joined together

$$u_\alpha^1 - e w_\alpha^1 = u_\alpha^2 \qquad (5)$$
$$w_i^1 = w_i^2$$

for displacement compatibility and

$$\begin{aligned} t_\alpha^1 + t_\alpha^2 &= 0 \\ p_3^1 + p_3^2 &= 0 \\ p_\alpha^1 - e t_\alpha^1 + p_\alpha^2 &= 0 \end{aligned} \qquad (6)$$

for equilibrium at the join line.

If there are two or more angled plates joined together (figure (3)), the approach proposed in [17, 14, 15] is followed. In order to simplify the description, the local coordinate systems for the M plates are assumed to be defined such that the x_2^m directions are all aligned with the same global direction along a straight join line.

The compatibility/equilibrium equations required along the join line are generated as follows. Each pair of plates (e.g. $m = 1$ and $m = 2$) deform compatibly: for each pair ($M = 2$) of angled plates joined together, the compatibility conditions can be enforced as follows:

$$\begin{aligned} (u_1^1 - e'_m w_1^1) n_{11}^1 + w_3^1 n_{13}^1 &= (u_1^2 - e'_k w_1^2) n_{11}^2 + w_3^2 n_{13}^2 \\ (u_1^1 - e'_m w_1^1) n_{31}^1 + w_3^1 n_{33}^1 &= (u_1^2 - e'_k w_1^2) n_{31}^2 + w_3^2 n_{33}^2 \\ u_2^1 &= u_2^2 \\ w_1^1 &= w_1^2 \\ w_2^1 &= 0 \\ w_2^2 &= 0 \end{aligned} \qquad (7)$$

where n_{ik}^m are the components of the rotation matrix of plate m from local to global coordinates. For M plates,

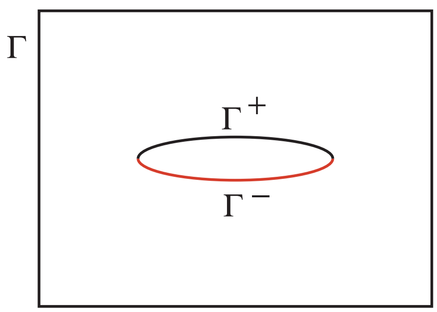

Figure 4: Crack geometry

equations (7) give $5M - 4$ compatibility conditions, which are supplemented by 4 equilibrium conditions:

$$\begin{aligned}\sum_{m=1}^{M}\{t_1^m n_{11}^m + p_3^m n_{13}^m\} = 0 \\ \sum_{m=1}^{M}(t_1^m n_{31}^m + p_3^m n_{33}^m) = 0 \\ \sum_{m=1}^{M} t_2^m = 0 \\ \sum_{m=1}^{M}(p_1^m - e'_m t_1^m) = 0\end{aligned} \tag{8}$$

where e'_m is the eccentricity of the m-plate respect to the centre of the joint. What is important is the relative eccentricity, therefore the reference point can be chosen arbitrarily. Usually, the quantities e'_m, and consequently the products $e'_m t_1^m$ are small compared to p_1^m, and for three or more angled plates can be ignored.

Dual boundary element method

The dual boundary element method was orginially formulated by Portela et al[47] and Mi and Aliabadi[38] for two and three-dimensional crack problems and later extended to plate bending by Dirgantara and Aliabadi[20, 18]. Consider a cracked plate as in figure (4), where Γ is the external boundary and Γ^+, Γ^- are the boundaries of the crack. Before deformation takes place, the boundaries Γ^+ and Γ^- are coincident. If equations (1) and (2) are applied on both boundaries, they result identical as shown in [4]. Another set of independent equations needs to be employed in order to build a non-singular system. Following [20] for plate problems, this extra set is provided by the boundary traction integral equations; these equations are found to be independent from the boundary displacement integral equations and can be applied to either of the crack boundaries.

The boundary traction integral equations can be derived by considering the equations that relate the stress resultants and the boundary tractions, as follows:

$$\begin{aligned} t_\alpha &= N_{\alpha\beta} n_\beta \\ p_3 &= Q_\alpha n_\alpha \\ p_\alpha &= M_{\alpha\beta} n_\beta \end{aligned} \tag{9}$$

By taking the integral expressions of the stress resultants to the boundary $((\mathbf{X}' \in \Omega) \longrightarrow \left(\mathbf{x}'_- \in \Gamma^-\right))$, considering that $(n_\beta(\mathbf{x}' \in \Gamma^+) = -n_\beta(\mathbf{x}' \in \Gamma^-))$ and assuming that Γ^- is smooth, they can be written as follows:

$$
\frac{1}{2}N_{\alpha\beta}(\mathbf{x}'_-) - \frac{1}{2}N_{\alpha\beta}(\mathbf{x}'_+) = \mathop{=\!\!\!\!\!\!\int} D^m_{\alpha\beta\gamma}(\mathbf{x}'_-, \mathbf{x})t_\gamma(\mathbf{x})d\Gamma - \int_\Gamma S^m_{\alpha\beta\gamma}(\mathbf{x}'_-, \mathbf{x})u_\gamma(\mathbf{x})d\Gamma \\
+ \int_\Omega D^m_{\alpha\beta\gamma}(\mathbf{x}'_-, \mathbf{X})f_\gamma(\mathbf{X})d\Omega \tag{10}
$$

for plate membrane, while for plate bending as:

$$
\frac{1}{2}M_{\alpha\beta}(\mathbf{x}'_-) - \frac{1}{2}M_{\alpha\beta}(\mathbf{x}'_+) = \mathop{=\!\!\!\!\!\!\int}_\Gamma D^b_{\alpha\beta k}(\mathbf{x}'_-, \mathbf{x})p_k(\mathbf{x})d\Gamma - \int_\Gamma S^b_{\alpha\beta k}(\mathbf{x}'_-, \mathbf{x})w_k(\mathbf{x})d\Gamma \\
+ \int_\Omega D^b_{\alpha\beta k}(\mathbf{x}'_-, \mathbf{X})q_k(\mathbf{X})d\Omega \\
\frac{1}{2}Q_{\beta}(\mathbf{x}'_-) - \frac{1}{2}Q_{\beta}(\mathbf{x}'_+) = \mathop{=\!\!\!\!\!\!\int}_\Gamma D^b_{3\beta k}(\mathbf{x}'_-, \mathbf{x})p_k(\mathbf{x})d\Gamma - \int_\Gamma S^b_{3\beta k}(\mathbf{x}'_-, \mathbf{x})w_k(\mathbf{x})d\Gamma \\
+ \int_\Omega D^b_{3\beta k}(\mathbf{x}'_-, \mathbf{X})q_k(\mathbf{X})d\Omega \tag{11}
$$

where the symbol $= \quad * -12pt \int$ stands for Hadamard principal value integral. The kernels $D^m_{\alpha\beta\gamma}, S^m_{\alpha\beta\gamma}, D^b_{\alpha\beta k}, S^b_{\alpha\beta k}, D^b_{3\beta k}$ and $S^b_{3\beta k}$ are linear combinations of the derivatives of the fundamental solutions and can be found in [18]. Kernels $D^b_{3\beta\gamma}$, $D^b_{3\beta\gamma}$ are weakly singular $O(\ln r)$; kernels $D^m_{\alpha\beta\gamma}$, $D^b_{\alpha\beta\gamma}$, $D^b_{3\beta 3}$, $S^b_{\alpha\beta 3}$, $S^b_{3\beta\gamma}$,have a strong (Cauchy principal value) singularity $O(1/r)$; $S^m_{\alpha\beta\gamma}$ are hyper-singular of the order $O(1/r^2)$ and kernels $S^b_{\alpha\beta\gamma}$, $S^b_{3\beta 3}$ are hyper-singular of the order $O(1/r^2 + \ln r)$. The integration techniques for these kernels can be found in [4].

Introducing equations (10)-(11) into (9), the boundary integral equations for tractions are obtained as follows:

$$
\frac{1}{2}t_\alpha(\mathbf{x}'_-) - \frac{1}{2}t_\alpha(\mathbf{x}'_+) = n_\beta(\mathbf{x}'_-) \mathop{=\!\!\!\!\!\!\int}_\Gamma D^m_{\alpha\beta\gamma}(\mathbf{x}'_-, \mathbf{x})t_\gamma(\mathbf{x})d\Gamma + \\
-n_\beta \int_\Gamma S^m_{\alpha\beta\gamma}(\mathbf{x}'_-, \mathbf{x})u_\gamma(\mathbf{x})d\Gamma + n_\beta \int_\Omega D^m_{\alpha\beta\gamma}(\mathbf{x}'_-, \mathbf{X})f_\gamma(\mathbf{X})d\Omega \tag{12}
$$

for plate membrane, while for plate bending as:

$$
\frac{1}{2}p_k(\mathbf{x}'_-) - \frac{1}{2}p_k(\mathbf{x}'_+) = n_\beta(\mathbf{x}'_-) \mathop{=\!\!\!\!\!\!\int}_\Gamma D^b_{k\beta k}(\mathbf{x}'_-, \mathbf{x})p_k(\mathbf{x})d\Gamma + \\
-n_\beta \int_\Gamma S^b_{k\beta k}(\mathbf{x}'_-, \mathbf{x})w_k(\mathbf{x})d\Gamma + n_\beta \int_\Omega D^b_{k\beta k}(\mathbf{x}', \mathbf{X})q_k(\mathbf{X})d\Omega \tag{13}
$$

The displacement integral equation for a source point $\mathbf{x}'_+ \in \Gamma^+$, can be written as follows:

$$
\frac{1}{2}u_\beta(\mathbf{x}'_+) - \frac{1}{2}u_\beta(\mathbf{x}'_-) + \fint T_{\alpha\beta}(\mathbf{x}'_+, \mathbf{x})u_\beta(\mathbf{x})d\Gamma = \\
\int_\Gamma U_{\alpha\beta}(\mathbf{x}'_+, \mathbf{x})t_\beta(\mathbf{x})d\Gamma + \int_\Omega U_{\alpha\beta}(\mathbf{x}'_+, \mathbf{X})f_\beta(\mathbf{X})d\Omega \tag{14}
$$

$$
\frac{1}{2}w_k(\mathbf{x}'_+) - \frac{1}{2}w_k(\mathbf{x}'_-) + \fint P_{ik}(\mathbf{x}'_+, \mathbf{x})w_k(\mathbf{x})d\Gamma = \\
\int_\Gamma W_{ik}(\mathbf{x}'_+, \mathbf{x})p_k(\mathbf{x})d\Gamma + \int_\Omega W_{ik}(\mathbf{x}'_+, \mathbf{X})q_k(\mathbf{X})d\Omega \tag{15}
$$

Equations (12)-(13) together with (14)-(15), form the required set of independent equations.

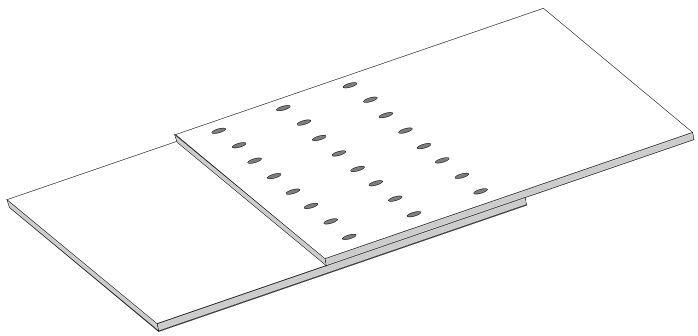

Figure 5: Two plates joined by rivets

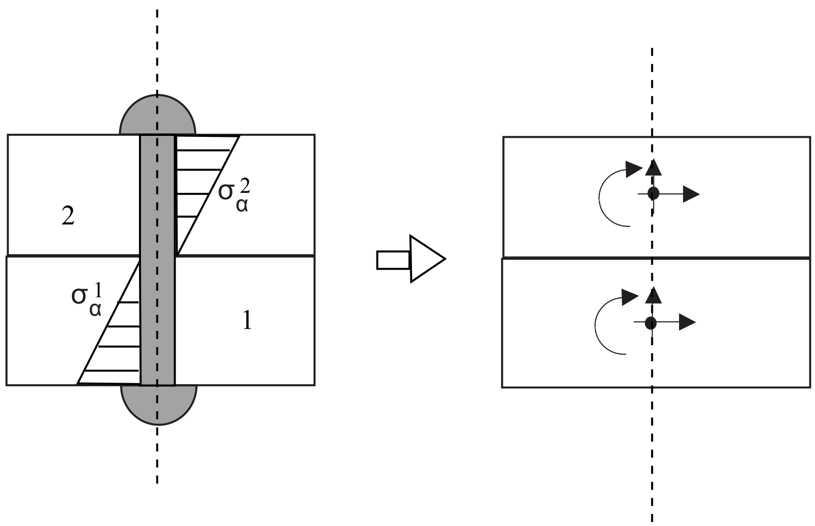

Figure 6: Rivet interaction forces

Boundary element formulation for riveted structures

Consider the geometry in figure (5) where two plates are joined together with rivets. Following Salgado and Aliabadi [52], each rivet is idealized as an attached point acting on the plates as an unknown domain point forces. Contact between the surfaces of the plates is not considered; thus they are modelled separately and they interact through unknown forces at rivet points. Being the rivets inserted in the plate, they generate moments with respect to the section of the plate; thus to the three forces along the main axis f_1^R, f_2^R, q_3^R two moments have to be added q_1^R and q_2^R, for a total of five unknown (see figure (6)) interaction forces for each attachment point.

For each plate considered separately, the following boundary displacement integral equations can be written:

$$C^m_{\alpha\beta}(\mathbf{x}')u_\beta(\mathbf{x}') + \int\!\!\!\!\!\!- T_{\alpha\beta}(\mathbf{x}', \mathbf{x})u_\beta(\mathbf{x})d\Gamma = \int_\Gamma U_{\alpha\beta}(\mathbf{x}', \mathbf{x})t_\beta(\mathbf{x})d\Gamma + \int_\Omega U_{\alpha\beta}(\mathbf{x}', \mathbf{X})f_\beta(\mathbf{X})d\Omega + \sum_R U_{\alpha\beta}(\mathbf{x}', \mathbf{x}_R)f^R_\beta(\mathbf{x}_R) \tag{16}$$

$$C^b_{ik}(\mathbf{x}')w_k(\mathbf{x}') + \int\!\!\!\!\!- P_{ik}(\mathbf{x}',\mathbf{x})w_k(\mathbf{x})d\Gamma = \tag{17}$$
$$\int_\Gamma W_{ik}(\mathbf{x}',\mathbf{x})p_k(\mathbf{x})d\Gamma + \int_\Omega W_{ik}(\mathbf{x}',\mathbf{X})q_k(\mathbf{X})d\Omega$$
$$+\sum_R W_{ik}(\mathbf{x}',\mathbf{x}_R)q^R_k(\mathbf{x}_R)$$

for a source point $\mathbf{x}' \in \Gamma$ (boundary of the plate), and for a rivet source point $\mathbf{x}'_R \in \Omega$ (domain of the plate):

$$u_\beta(\mathbf{x}'_R) + \int\!\!\!\!\!- T_{\alpha\beta}(\mathbf{x}'_R,\mathbf{x})u_\beta(\mathbf{x})d\Gamma = \tag{18}$$
$$\int_\Gamma U_{\alpha\beta}(\mathbf{x}'_R,\mathbf{x})t_\beta(\mathbf{x})d\Gamma + \int_\Omega U_{\alpha\beta}(\mathbf{x}'_R,\mathbf{X})f_\beta(\mathbf{X})d\Omega +$$
$$+\sum_R U_{\alpha\beta}(\mathbf{x}'_R,\mathbf{x}_R)f^R_\beta(\mathbf{x}_R)$$

$$w_k(\mathbf{x}'_R) + \int\!\!\!\!\!- P_{ik}(\mathbf{x}'_R,\mathbf{x})w_k(\mathbf{x})d\Gamma = \tag{19}$$
$$\int_\Gamma W_{ik}(\mathbf{x}'_R,\mathbf{x})p_k(\mathbf{x})d\Gamma + \int_\Omega W_{ik}(\mathbf{x}'_R,\mathbf{X})q_k(\mathbf{X})d\Omega +$$
$$+\sum_R W_{ik}(\mathbf{x}'_R,\mathbf{x}_R)q^R_k(\mathbf{x}_R)$$

where $\mathbf{x}_R$ are rivet points, and the summations are extended to R rivets. The quantities u_β, w_k, t_β and p_k are displacements, rotations, moments and tractions at the boundary of the plate; f_β and q_k are domain loads; f^R_β and q^R_k are rivet forces and moments; $T_{\alpha\beta}(\mathbf{X}',\mathbf{X})$, $U_{\alpha\beta}(\mathbf{X}',\mathbf{X})$, $P_{ik}(\mathbf{X}',\mathbf{X})$ and $W_{ik}(\mathbf{X}',\mathbf{X})$ are the fundamental solutions for plate membrane and plate bending respectively. The evaluation of kernels, coefficients and limiting processes can be found in [4]. All known domain loads are transferred to the boundary by means of the DRM.

As pointed out in [52], when evaluating the kernels at a rivet point they present some singularity (W_{ik} and $U_{\alpha\beta}$ are weakly singular of order $O(\ln r)$). In order to overcome the problem the method proposed by Poe [43] is used. The rivet load is considered to be uniformly distributed along a line segment, perpendicular to the force and centred at the application point. The length of the line is taken as the rivet diameter; then the singular kernels can be calculated using special integration techniques accordingly to the singularity.

Rivet model

For each rivet there are 10 additional unknowns for each plate, five forces and five displacements; the additional integral equations are five for each rivet for each plate, therefore: $2R(10-5) = 10R$. Ten extra equations for each rivet are needed, and these can be found enforcing compatibility and equilibrium conditions at the rivet points. Consider the geometry in figure (7); it represents the section of a typical plate-rivet-plate attachment.

The equilibrium conditions for the rivet can be written as follows:

$$f^R_\beta(1) + f^R_\beta(2) = 0 \tag{20}$$
$$q^R_3(1) + q^R_3(2) = 0$$

for the equilibrium along the main axis; the equilibrium of the moments is enforced respect to the point of the rivet laying on the interface between the two plates as follows:

$$q^R_\beta(1) - \frac{h^1}{2}f^R_\beta(1) + q^R_\beta(2) + \frac{h^2}{2}f^R_\beta(2) = 0 \tag{21}$$

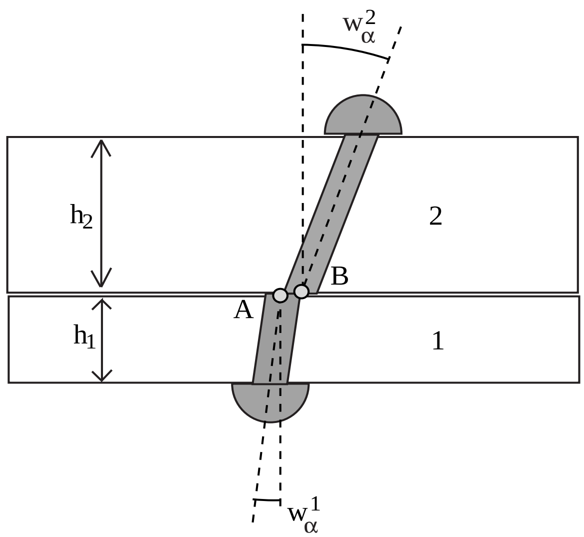

Figure 7: Typical section of plate-rivet-plate attachment

where the index 1 and 2 are referred to the lower and upper plate respectively.

For what concern the compatibility equations, the flexibility of the rivet has to be considered. At point A and B, the displacements are related as follows:

$$\begin{aligned} u_\alpha^R(1) + \frac{h^1}{2} w_\beta^R(1) - u_\alpha^R(2) + \frac{h^2}{2} w_\beta^R(2) = \Phi^R f_\beta^R(1) \\ w_3^R(1) - w_3^R(2) = 0 \end{aligned} \tag{22}$$

where Φ^R is the rivet flexibility and depends on the rivet material and geometrical properties. The rivet flexibility Φ^R can affect considerably the results. Several empirical formulas have been proposed, and some are listed in [39, 43, 61].

The difference between the rotation of the two part in which the rivet is divided, can be related to the flexibility of each part considered on its own, as follows:

$$\begin{aligned} w_\beta^R(1) - w_\beta^R(2) = \\ \frac{64}{E_R \pi D_R^4} \left[\frac{1}{h^1} \left(q_\beta^R(1) - \frac{h^1}{2} f_\beta^R(1) \right) + \frac{1}{h^2} \left(q_\beta^R(2) + \frac{h^2}{2} f_\beta^R(2) \right) \right] \end{aligned} \tag{23}$$

where E_R, D_R are the Young's modulus and diameter of the rivet respectively, and $\pi D_R^4 h^\alpha/64$ are the inertia momentum of the two part of the rivet of circular cross section. If the plates have the same thickness, equation (23) reduce to:

$$w_\beta^R(1) - w_\beta^R(2) = 0 \tag{24}$$

Dual boundary integral equations for riveted patches

A patch riveted to an undamaged plate can be treated as two plates riveted together and equations (16)-(19) can be employed. If a crack is introduced, traction boundary integral equations onto one of the crack surfaces need to be applied. Following the same reasoning as for equations (12)-(13), the traction boundary integral equations for riveted patches can be written as follows:

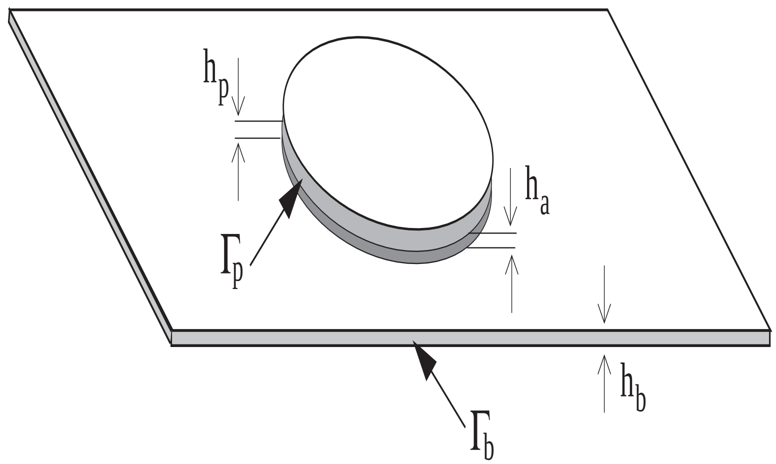

Figure 8: Adhesively bonded patch

$$t_\alpha(\mathbf{x}'_-) = n_\beta \fint_\Gamma D^m_{\alpha\beta\gamma}(\mathbf{x}'_-,\mathbf{x})t_\gamma(\mathbf{x})d\Gamma - n_\beta \int_\Gamma S^m_{\alpha\beta\gamma}(\mathbf{x}'_-,\mathbf{x})u_\gamma(\mathbf{x})d\Gamma \tag{25}$$
$$+n_\beta \int_\Omega D^m_{\alpha\beta\gamma}(\mathbf{x}'_-,\mathbf{X})f_\gamma(\mathbf{X})d\Omega + \sum_R n_\beta D^m_{\alpha\beta\gamma}(\mathbf{x}'_-,\mathbf{x}_R)f^R_\beta(\mathbf{x}_R)$$

for membrane, and for bending as:

$$p_k(\mathbf{x}'_-) = n_\beta \fint_\Gamma D^b_{k\beta k}(\mathbf{x}'_-,\mathbf{x})p_k(\mathbf{x})d\Gamma - n_\beta \int_\Gamma S^b_{k\beta k}(\mathbf{x}'_-,\mathbf{x})w_k(\mathbf{x})d\Gamma \tag{26}$$
$$+n_\beta \int_\Omega D^b_{k\beta k}(\mathbf{x}'_-,\mathbf{X})q_k(\mathbf{X})d\Omega + \sum_R n_\beta D^b_{k\beta k}(\mathbf{x}'_-,\mathbf{x}_R)q^R_k(\mathbf{x}_R)$$

where R is the number of rivet points; the kernels $D^m_{\alpha\beta\gamma}$, $S^m_{\alpha\beta\gamma}$, and $D^b_{i\beta k}$, $S^b_{i\beta k}$ have been already defined and their expressions can be found in Appendix A. It has to be noticed that source points of equations (25)-(26) are never on rivet points, therefore the kernel in the summatory are not singular.

Boundary integral equations for adhesively bonded patches

Consider a plate with a patch as in figure (8), where Γ^b and Ω^b are the boundary and the domain of the plate; Γ^p and Ω^p are the boundary and the domain of the patch and h_b, h_p and h_a are the thicknesses of the plate, the patch and of the adhesive layer respectively. The plate and patch interact through the adhesive layer by means of body forces, which follow the bonding conditions. Following Goland and Reissner [24], the adhesive layer and the adherends interact through shear and peel stress $(\sigma_\alpha, \sigma_3)$. As illustrated in figure (9), the shear stresses are applied on the the upper and lower surfaces, therefore they generate moments with respect to the mid-surface of

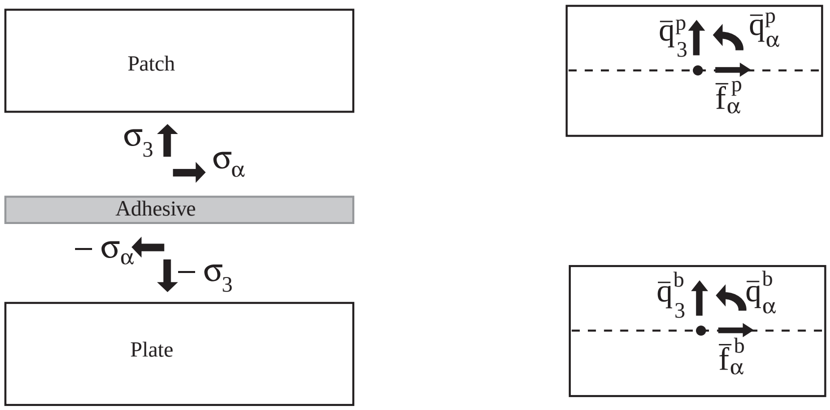

Figure 9: Interaction forces for the adhesively bonded plates

the adhesive and adherends. The resulting body forces acting on the adherends can be summarized as in-plane $\bar{f}_\alpha^b$, $\bar{f}_\alpha^p$, transverse $\bar{q}_\alpha^b$, $\bar{q}_\alpha^p$ and moment $\bar{q}_\alpha^b$, $\bar{q}_\alpha^p$ body forces, for plate and patch respectively. These body forces are unknowns of the problems, five for each set of equations, and need to be calculated. For a generic adhesively bonded point, five compatibility and five equilibrium equations can be derived from equilibrium and geometrical considerations. From equilibrium conditions along the main axis the following equations can be written:

$$\begin{aligned} \bar{f}_\alpha^p + \bar{f}_\alpha^b &= 0 \\ \bar{q}_3^p + \bar{q}_3^b &= 0 \end{aligned} \tag{27}$$

and considering the equilibrium of the moments with respect to the mid-plane of the adhesive:

$$\bar{q}_\alpha^p - \bar{f}_\alpha^p \frac{h_p + h_a}{2} + \bar{q}_\alpha^b + \bar{f}_\alpha^b \frac{h_b + h_a}{2} = 0 \tag{28}$$

Considering negligible the strain across the adhesive, for in-plane displacements and deflections at points A and B the following compatibility conditions can be written:

$$\begin{gathered} \bar{u}_\alpha^p - \bar{w}_\alpha^p \frac{h_p}{2} - \bar{u}_\alpha^b - \bar{w}_\alpha^b \frac{h_b}{2} = \frac{h_a}{G_a} \bar{f}_\alpha^p \\ w_3^p - w_3^b = 0 \end{gathered} \tag{29}$$

where G_α is the shear modulus of the adhesive.

The difference between the rotations of each adherend, can be related to the flexibility of each adherend, as follows:

$$w_\alpha^b - w_\alpha^p = \left(\frac{12}{E_b h_b^3} - \frac{12}{E_p h_p^3} \right) \left(\bar{q}_\alpha^b + \bar{f}_\alpha^b \frac{h_b + h_a}{2} \right) \tag{30}$$

If plate and patch are made of the same material ($E_p = E_b$) and have same thicknesses ($h_p = h_b$), equation (30) reduces to:

$$w_\alpha^b - w_\alpha^p = 0 \tag{31}$$

Equations (27-30) form a complete set of bonding conditions. It has to be noticed that equation (30) allows different rotations for plate and patches, differently from what proposed in [71].

For what concerns the boundary element formulation, an approach similar to what suggested in [53] for 2D and extended to plates in [71] will be followed here.

Considering P patches and that $\Omega^p \subset \Omega^b$ (in plate theory, plate and patches lay on the same plane), the displacement boundary integral equations for the plate and the patches can be written as follows:

$$\begin{gathered} C_{\alpha\beta}(\mathbf{x}')u_\beta(\mathbf{x}') + \fint T_{\alpha\beta}(\mathbf{x}',\mathbf{x})u_\beta(\mathbf{x})d\Gamma = \\ \int_\Gamma U_{\alpha\beta}(\mathbf{x}',\mathbf{x})t_\beta(\mathbf{x})d\Gamma + \int_\Omega U_{\alpha\beta}(\mathbf{x}',\mathbf{X})f_\beta(\mathbf{X})d\Omega + \\ + \sum_P \int_{\Omega_p} U_{\alpha\beta}(\mathbf{x}',\mathbf{X}_p)\bar{f}_\beta(\mathbf{X}_p) \end{gathered} \tag{32}$$

for membrane, and for bending as:

$$\begin{gathered} C_{ik}(\mathbf{x}')w_k(\mathbf{x}') + \fint P_{ik}(\mathbf{x}',\mathbf{x})w_k(\mathbf{x})d\Gamma = \\ \int_\Gamma W_{ik}(\mathbf{x}',\mathbf{x})p_k(\mathbf{x})d\Gamma + \int_\Omega W_{ik}(\mathbf{x}',\mathbf{X})q_k(\mathbf{X})d\Omega \\ + \sum_P \int_{\Omega_p} W_{ik}(\mathbf{x}',\mathbf{X}_p)\bar{q}_k(\mathbf{X}_p) \end{gathered} \tag{33}$$

where $\Gamma = \Gamma^p, \Gamma^b$, $\Omega = \Omega^p, \Omega^b$, $\bar{f}_\beta = \bar{f}^p_\alpha, \bar{f}^b_\alpha$ and $\bar{f}_\beta = \bar{f}^p_\alpha, \bar{f}^b_\alpha$ whether equations are written for the plate or for the patches. The other quantities follow definitions given before. All the domain integrals in equations (32)-(33) are transferred to the boundary by means of DRM. The mutual contribution between plate and patch is exercised through N_p bonding point, which are treated as DRM points collocated within the plate and patch domains; compatibility and equilibrium conditions as described by equations (27)-(30) are then enforced between plate and patch points. For each bonding point the displacement integral equations can be written as follows:

$$\begin{gathered} u_\beta(\mathbf{x}') + \fint T_{\alpha\beta}(\mathbf{x}',\mathbf{x})u_\beta(\mathbf{x})d\Gamma = \\ \int_\Gamma U_{\alpha\beta}(\mathbf{x}',\mathbf{x})t_\beta(\mathbf{x})d\Gamma + \int_\Omega U_{\alpha\beta}(\mathbf{x}',\mathbf{X})f_\beta(\mathbf{X})d\Omega + \\ + \sum_P \int_{\Omega_p} U_{\alpha\beta}(\mathbf{x}',\mathbf{X}_p)\bar{f}_\beta(\mathbf{X}_p) \end{gathered} \tag{34}$$

for membrane, and for bending as:

$$\begin{gathered} w_k(\mathbf{x}') + \fint P_{ik}(\mathbf{x}',\mathbf{x})w_k(\mathbf{x})d\Gamma = \\ \int_\Gamma W_{ik}(\mathbf{x}',\mathbf{x})p_k(\mathbf{x})d\Gamma + \int_\Omega W_{ik}(\mathbf{x}',\mathbf{X})q_k(\mathbf{X})d\Omega \\ + \sum_P \int_{\Omega_p} W_{ik}(\mathbf{x}',\mathbf{X}_p)\bar{q}_k(\mathbf{X}_p) \end{gathered} \tag{35}$$

where the symbols have been already defined.

Dual boundary integral equations for adhesively bonded patches

Displacement boundary integral equations (32)-(33) are applied to one surfaces and traction integral equations to the other. The latter can be derived in a similar way as described before, and can be written as follows:

$$
\begin{aligned}
t_\alpha(\mathbf{x}'_-) = n_\beta \fint_{\Gamma^b} D^m_{\alpha\beta\gamma}(\mathbf{x}'_-,\mathbf{x}) t_\gamma(\mathbf{x}) d\Gamma - n_\beta \int_{\Gamma^b} S^m_{\alpha\beta\gamma}(\mathbf{x}'_-,\mathbf{x}) u_\gamma(\mathbf{x}) d\Gamma \\
+ n_\beta \int_{\Omega^b} D^m_{\alpha\beta\gamma}(\mathbf{x}'_-,\mathbf{X}) f_\gamma(\mathbf{X}) d\Omega + \sum_P n_\beta \int_{\Omega_p} D^m_{\alpha\beta\gamma}(\mathbf{x}'_-,\mathbf{X}_p) \bar{f}_\gamma(\mathbf{X}_p)
\end{aligned}
\tag{36}
$$

for membrane, and for bending as:

$$
\begin{aligned}
p_k(\mathbf{x}'_-) = n_\beta \fint_{\Gamma^b} D^b_{k\beta k}(\mathbf{x}'_-,\mathbf{x}) p_k(\mathbf{x}) d\Gamma - n_\beta \int_{\Gamma^b} S^b_{k\beta k}(\mathbf{x}'_-,\mathbf{x}) w_k(\mathbf{x}) d\Gamma \\
+ n_\beta \int_{\Omega^b} D^b_{k\beta k}(\mathbf{x}'_-,\mathbf{X}) q_k(\mathbf{X}) d\Omega + \sum_P n_\beta \int_{\Omega_p} D^b_{k\beta k}(\mathbf{x}'_-,\mathbf{X}_p) \bar{q}_k(\mathbf{X}_p)
\end{aligned}
\tag{37}
$$

where all the quantities have been already defined previously. It has to be noticed that equations (36)-(37) are applied to the plate and not to the patch.

System matrix

Each plate and patch are discretized into boundary and DRM points. The latter may be considered either as normal DRM, rivet or bonding points, accordingly to the case in exam. The system for a plate joined through edges to another plate, and with rivets and adhesive points can written in matrix form as follows:

$$
\begin{array}{r|c|c|c|c|c|c|c|c|c|c|c|}
 & ds.b. & t.b. & ds.j & ds.d & ds.a. & ds.r & t.j & t.a & t.r & & d.load. \\
\hline
b.eq. & H_{bd} & G_{bd} & H_{bj} & 0 & 0 & 0 & G_{bj} & E_{ba} & G_{br} & & F_{bd} \\
\hline
d.eq. & H_{db} & G_{db} & H_{dj} & I_{dd} & 0 & 0 & G_{dj} & E_{da} & G_{dr} & = & F_{dd} \\
\hline
a.eq. & H_{ab} & G_{ab} & H_{aj} & 0 & I_{aa} & 0 & G_{aj} & E_{aa} & G_{ar} & & F_{ad} \\
\hline
r.eq & H_{rb} & G_{rb} & H_{rj} & 0 & 0 & I_{rr} & G_{rj} & E_{ra} & G_{rr} & & F_{rd} \\
\hline
\end{array}
\tag{38}
$$

where suffix b, d, j, a and r stay for boundary, domain, join-line, bonding and rivet points respectively. H are the integrals computed from traction fundamental solutions, G from displacement fundamental solutions, E from DRM and I is the identity matrix; F are the domain load contributions of the prescribed loads evaluated with DRM. For example the term H_{aj} is the coefficient computed using the traction fundamental solution with bonding points as source points and join-lines points as field points, and they correspond to the join-line displacements contribution to the bonding point displacements. After boundary conditions are imposed and considering the general case, where plates are riveted or joined along the edges, and there are bonded patches; the resulting system can be written in matrix form as follows:

$$
\begin{array}{|c|c|c|c|c|c|}
\hline
.. & 0 & 0 & 0 & 0 & 0 \\ \hline
0 & A^i & 0 & 0 & 0 & 0 \\ \hline
0 & 0 & A^p & 0 & 0 & 0 \\ \hline
0 & 0 & 0 & A^j & 0 & 0 \\ \hline
0 & 0 & 0 & 0 & .. & 0 \\ \hline
0 & 0 & 0 & 0 & 0 & A^k \\ \hline
0 & P^{ip} & P^{ip} & 0 & 0 & 0 \\ \hline
0 & 0 & 0 & J^{jk} & 0 & J^{jk} \\ \hline
0 & R^{ij} & 0 & R^{ij} & 0 & 0 \\ \hline
\end{array}
=
\begin{array}{|c|}
\hline
.. \\ \hline F^i \\ \hline F^j \\ \hline F^j \\ \hline .. \\ \hline F^k \\ \hline 0 \\ \hline 0 \\ \hline 0 \\ \hline
\end{array}
+
\begin{array}{|c|}
\hline
.. \\ \hline b^i \\ \hline b^j \\ \hline b^j \\ \hline .. \\ \hline b^k \\ \hline 0 \\ \hline 0 \\ \hline 0 \\ \hline
\end{array}
\tag{39}
$$

where A^j and F^j are the matrix of coefficient and the load vector of the j plate; J^{jk} are the matrix containing the joining conditions between plates j and k, supposed that they are joined along edges; R^{ij} are the matrix containing the joining conditions between plates i and j, supposed they are connected with rivets, and P^{ip} are the matrix containing the joining conditions between plate i and patch p, supposed they are adhesively bonded. Vectors F^i contain the prescribed domain loads contributions, while b^i correspond to the known boundary values.

Evaluation of the fracture parameters

Following [20], the SIFs can be expressed in terms of displacements discontinuities at crack boundaries as:

$$\left\{\begin{array}{c} K_1^m \\ K_2^m \\ K_1^b \\ K_2^b \\ K_3^b \end{array}\right\} = \frac{1}{\sqrt{r}} \left[\begin{array}{ccccc} \frac{Eh}{8}\sqrt{2\pi} & 0 & 0 & 0 & 0 \\ 0 & \frac{Eh}{8}\sqrt{2\pi} & 0 & 0 & 0 \\ 0 & 0 & \frac{Eh^3}{48}\sqrt{\frac{\pi}{2}} & 0 & 0 \\ 0 & 0 & 0 & \frac{Eh^3}{48}\sqrt{\frac{\pi}{2}} & 0 \\ 0 & 0 & 0 & 0 & \frac{5Eh}{24(1+\upsilon)}\sqrt{\frac{\pi}{2}} \end{array}\right] \left\{\begin{array}{c} \Delta u_1 \\ \Delta u_2 \\ \Delta w_1 \\ \Delta w_2 \\ \Delta w_3 \end{array}\right\} \tag{40}$$

where $\Delta u_\alpha, \Delta w_i$ are defined as:

$$\begin{gathered} \Delta u_\alpha(\mathbf{x}) = u_\alpha(\mathbf{x}^+) - u_\alpha(\mathbf{x}^-) \\ \Delta w_i(\mathbf{x}) = w_i(\mathbf{x}^+) - w_i(\mathbf{x}^-) \\ \left(\mathbf{x}^+ \in \Gamma^+; \mathbf{x}^- \in \Gamma^-\right) \end{gathered} \tag{41}$$

The effective value of SIFs is extrapolated from the values at nodes of crack tip elements using the Displacement Extrapolation Method as described in [4].

The $J-integral$ can be written separately for plate membrane and bending [19] as follows:

$$J^m = \int_\Gamma \left[N_{\alpha\beta}\frac{1}{2}\left(u_{\alpha,\beta} + u_{\beta,\alpha}\right)n_n - t_\beta u_{\beta,n}\right]d\Gamma - \int_\Omega f_\beta u_{\beta,n} d\Omega \tag{42}$$

and for bending:

$$\begin{gathered} J^b = \int_\Gamma \left[\left(Q_\alpha\left(w_\alpha + w_{3,\alpha}\right) + M_{\alpha\beta}\frac{1}{2}\left(w_{\alpha,\beta} + w_{\beta,\alpha}\right)\right)n_n + \right. \\ \left. -p_k w_{k,n} d\Gamma\right] - \int_\Omega q_k w_{k,n} d\Omega \end{gathered} \tag{43}$$

where J^m and J^b stand for membrane and bending $J-integral$ respectively, and the can be related to the stress resultant intensity factors as follows:

$$\begin{gathered} J^m = \frac{(1-\nu^2)}{E}\left(K_{1m}^2 + K_{2m}^2\right) \\ J^b = \frac{12}{Eh^3}\left[K_{1b}^2 + K_{2b}^2 + \frac{(1+\nu)}{\lambda^2}K_{3b}^2\right] \end{gathered} \tag{44}$$

In order to extract the SIFs for each mode independently, the separation technique proposed by Rigby and Aliabadi [51] for 3D, and by Dirgantara and Aliabadi for plates [19] is followed. The principle of the method lays in the possibility of decomposing the stress-strain field ahead of the crack-tip into symmetric and anti-symmetric fields, and then relating these to the different crack deformation modes.

The stress resultant intensity factors can be related to the standard stress intensity factors (SIFs) as follows:

$$\begin{gathered} K_I = \frac{K_{1m}}{h} + K_{1b}\frac{12}{h^3}z \\ K_{II} = \frac{K_{2m}}{h} + K_{2b}\frac{12}{h^3}z \\ K_{III} = \frac{3}{2h}K_{3b}\left(1 - \left(\frac{2z}{h}\right)^2\right) \end{gathered} \tag{45}$$

where z is the coordinate that runs along the thickness (h) of the plate.

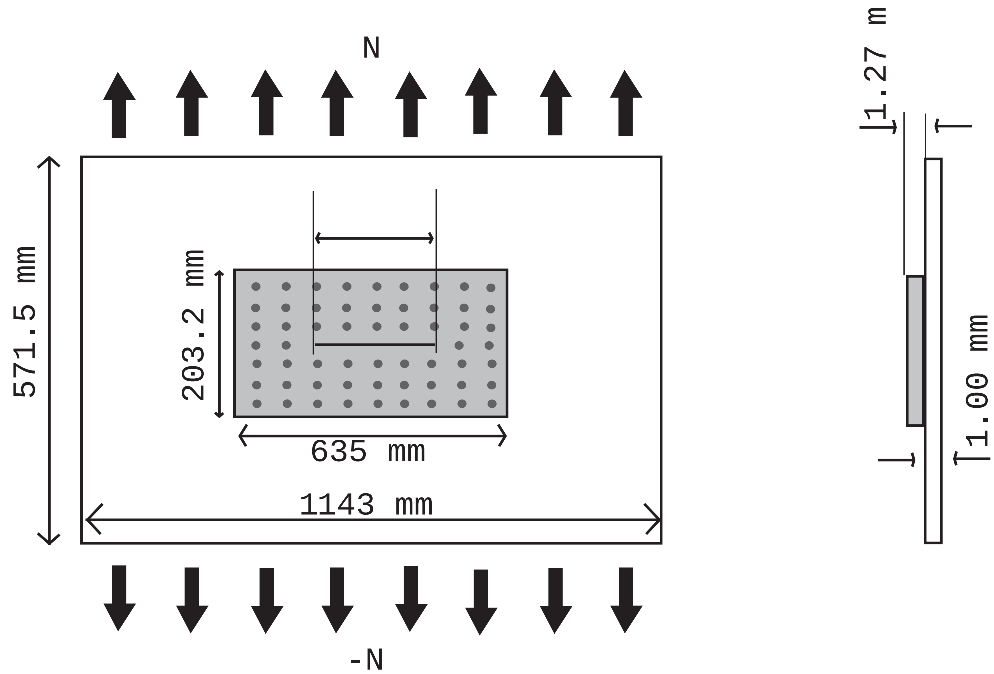

Figure 10: Cracked sheet with rectangular patch: geometry and load

Examples

Cracked sheet reinforced with a riveted rectangular patch

In figure (10) a cracked sheet with a riveted rectangular patch is presented. Material properties for the sheet and the patch are: Young modulus $E = 68900MPa$, Poisson's ratio $\nu = 0.33$. Dimensions are given in the same figure. The patch is attached with 200 rivets of diameter $D_R = 4.76mm$, and which material properties are the same as for the sheet and the patch. Rivets are regularly distributed in eight rows of 25 rivets each, with a pitch $p = 25.4mm$. The sheet is modelled with 64 boundary elements (32 on the outer boundary and 32 on the crack), while 32 boundary elements only are used for the patch. In figure (11), the by-pass load ratio (F_x/N) is plotted for different rivet rows. Results are compared with [75] and are found to be in good agreement.

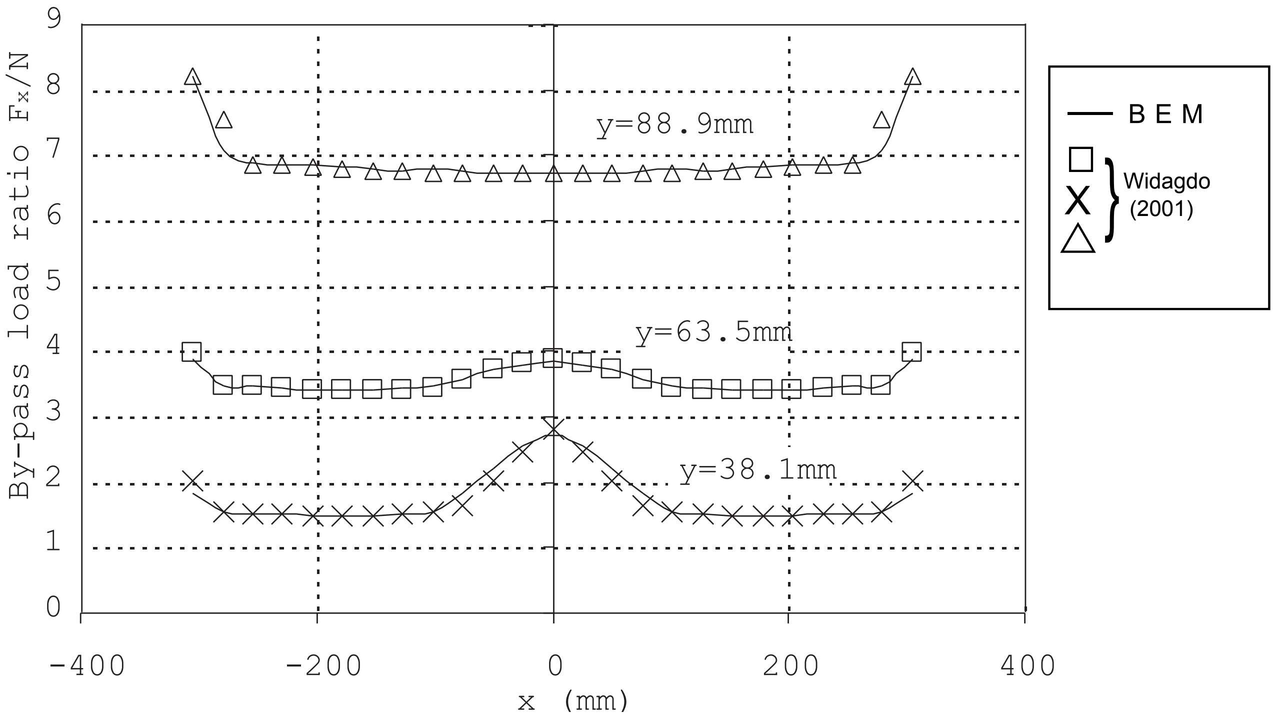

Figure 11: Cracked sheet with rectangular patch: By-pass load ratio

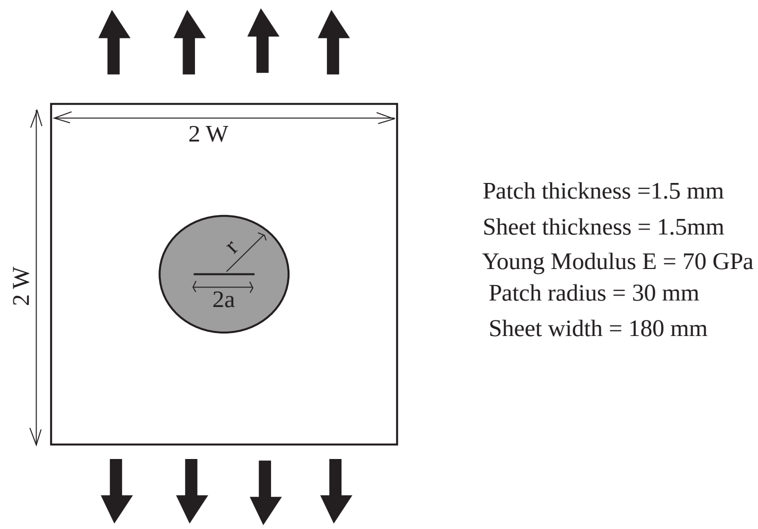

Figure 12: Cracked plate with a circular patch

Cracked sheet reinforced with a circular doubler attached with rivets or adhesive

Consider a cracked plate as illustrated in figure (12). The plate is square ($2W = 180mm$), with a central crack of various size ($2a$). Two opposite edge are loaded with in plane normal stress resultant N_{yy} which generate a stress $\sigma_{yy} = 100MPa$, and a circular patch of radius $r = 30mm$ is attached as shown. Material properties of the plate and the patch are those of Aluminium (Young's modulus $E = 70GPa$, Poisson's ratio $\nu = 0.3$) and both have thickness $h = 1.5mm$. The plate and the patch are modelled with 16 boundary elements each, while for the crack 8 discontinuous boundary elements are used on each surface. First the plate without crack and with the patch is modeled in three different ways, as illustrated in figure (13). A solid model (perfect bonding) of the patch as a central circular plate of thickness $h_s = 2h$ is joined through the edge with eccentricity $e = 0.75mm$; riveted patch with 12 rivets of same material properties as the plate and the patch, with diameter $D_R = 7mm$; and an adhesively bonded patch with adhesive thickness $h_a = 0.15mm$ and shear modulus $G_a = 0.6GPa$.

The deflection w at the centre of the patch are presented in table (1). Convergence for the adhesive patch have been reached with few bonding points, nevertheless 76 points have been placed as the crack results converged for this value. It can be noticed how the adhesive solution is close to the solid model, while the rivet model present the highest deflection. The by-pass load ($N_{yy}/N_{applied}$) is about 17% for the rivet model and 13% for the adhesive model. Higher loads in the patch generate higher moments which cause the plate deflection.

	PFB	Adh	Riv
w	-3.50	-3.55	-3.99

Table 1: Cracked plate with a circular patch: maximum deflection comparison

The crack is then introduced, and SIF ratio $K_I/\sigma_{applied}$ for membrane and bending against half crack size a are presented in figures (14)-(15). The behaviour of $K_{1m}/\sigma_{applied}$ is compared with the un-patched plate. Results from Murakami [40] are compared with the un-patched BEM model and they match perfectly. The riveted patch improve the situation, but not as much as the bonded patch, for which an average reduction of about 3 times is observed for all crack sizes. It has to be noticed that the patch induce bending thus bending stress resultant intensity factors are found as well for the patched models. For comparison results presented

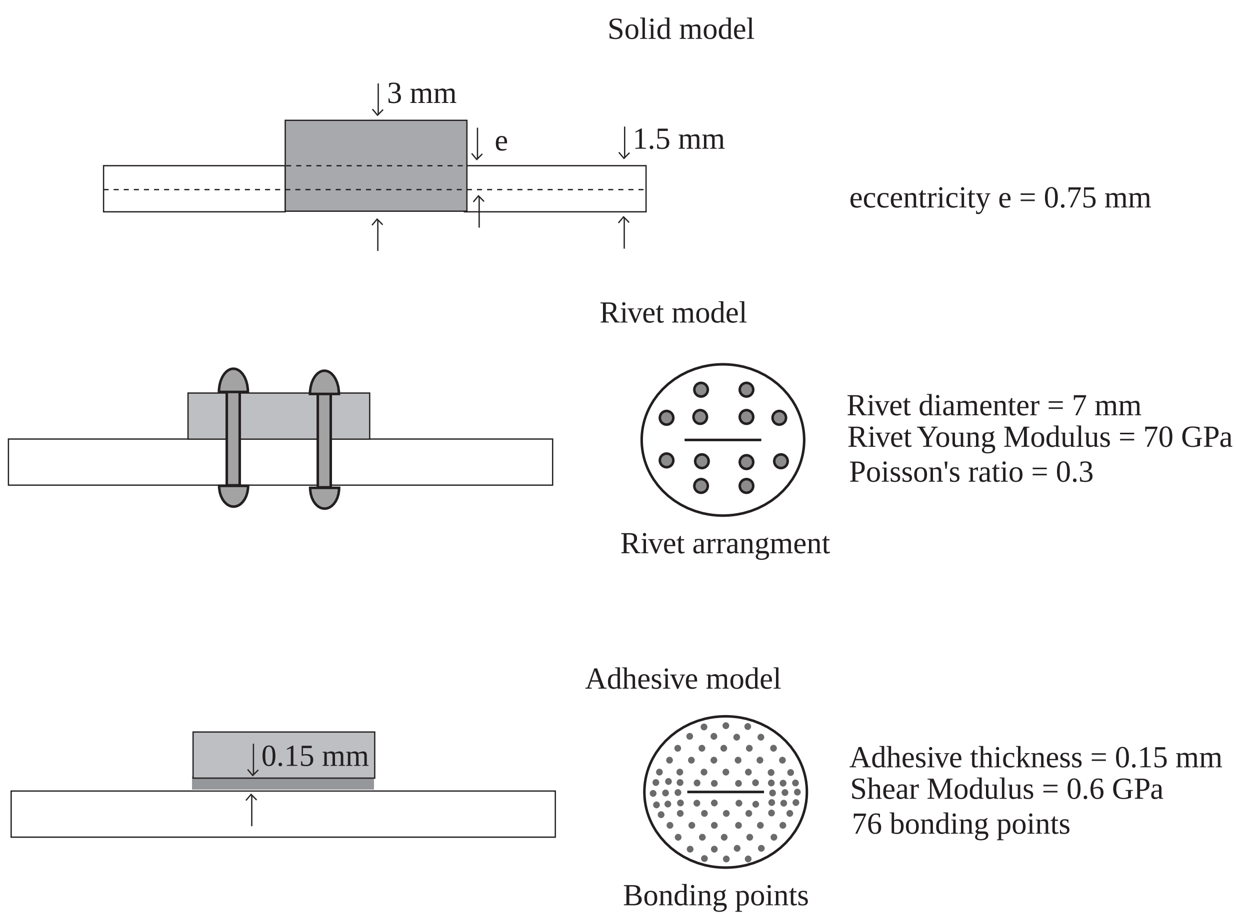

Figure 13: Different patch attachment models

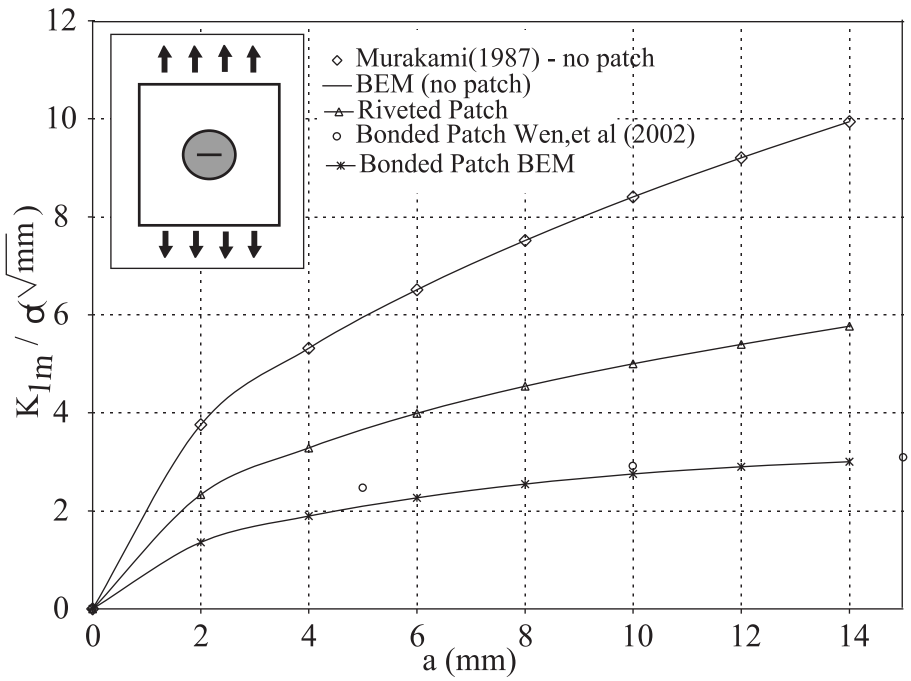

Figure 14: Single plate: SIF mode I membrane against half crack size a

by Wen, Aliabadi and Young in [71] are presented as well; it can be seen how they are in good agreement apart for small crack size. This is probably due to the different adhesive models; present formulation allows relative rotations between plate and patch. The difference is even more clear in figure (15) where $K_{1b}/\sigma_{applied}$ are plotted against half crack size a for riveted and bonded patch. It can be seen how in [71], $K_{1b}/\sigma_{applied}$ remains almost constant, while it is growing with crack size, both for bonded and riveted. The condition of same rotations probably reduces the flexural rigidity of the joint. If maximum SIF are considered, the reduction for the bonded patch is 4.5 with respect to the un-patched plate; this result is in accordance with [8].

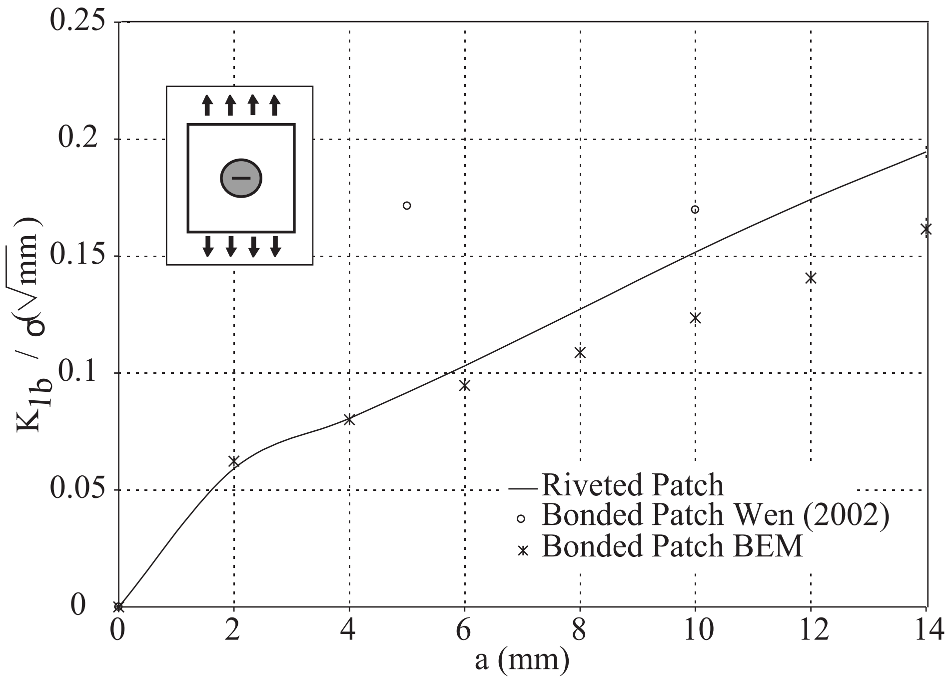

Figure 15: Single plate: SIF mode I bending against half crack size a

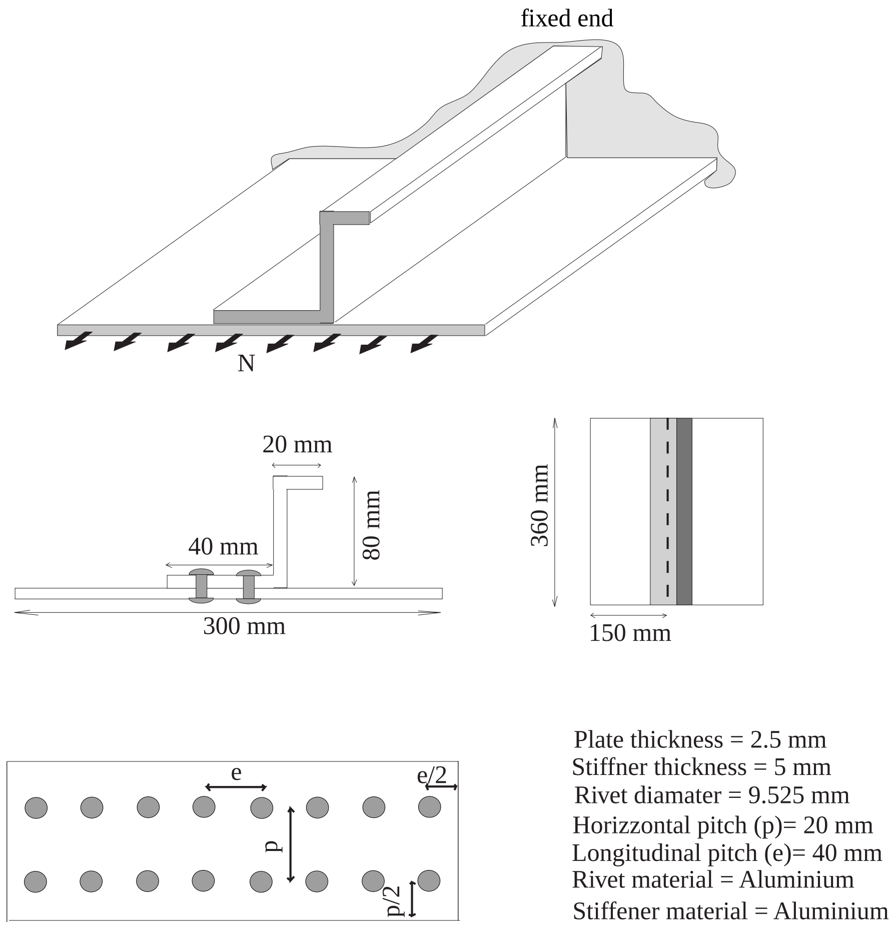

Figure 16: Stiffener riveted to plate: geometry and load

Adhesive patching of a cracked stiffened plate

Consider the stiffener-plate structure illustrated in figure (16). A Z-stiffener is attached to a plate with 16 rivets as shown. Material properties of the stiffener and the plate are those of Aluminium (Young's modulus $E = 73GPa$ and Poisson's ratio $\nu = 0.3$); the plate thickness is $2.5mm$ while the stiffener is made of plates $5mm$ thick, joined through the edge. Material properties of the rivets are the same as plate and stiffener, rivets diameter is $D_R = 9.525mm$. Each plate is modelled with 16 boundary elements. The piece is fixed at one end and the plate is loaded with tension $N = 100N/mm$ on the opposite edge. Suppose that the two correspondent rivets at fifth place from the fixed edge fail and a crack is placed instead, of initial size $c = 20mm$. Equal cracks are present both in the plate and the stiffener and grow. In figure (17) is shown how they are considered; the crack in the plate grows normally, while the crack in the stiffener grows initially in the lower part, then reach the edge of the stiffener on one side and breaks through the vertical plate on the other side. Eventually, when the crack in plate reaches $c = 160mm$, the stiffener is considered to be broken off. The growth of the cracks is considered happening at the same time. Then the repaired structure is considered.

A rectangular patch of size (180×90) and thickness $2.5mm$ is attached onto the crack. The patch is made of Aluminium and is modelled with 16 boundary elements, and 79 bonding points are regularly placed in the bonded area. The broken stiffener is replaced. In figure (18) the repaired structure is illustrated. In figure (19) results for maximum mode I SIF are presented for all cases. Analyzing the broken structure first, for the plate three different areas can be recognized. First, for $10mm \le c \le 40mm$ rather low $K_I^{\max}$ are found; the stiffener is still helping in carrying the load. Secondly, when the crack eventually grows out of the stiffener

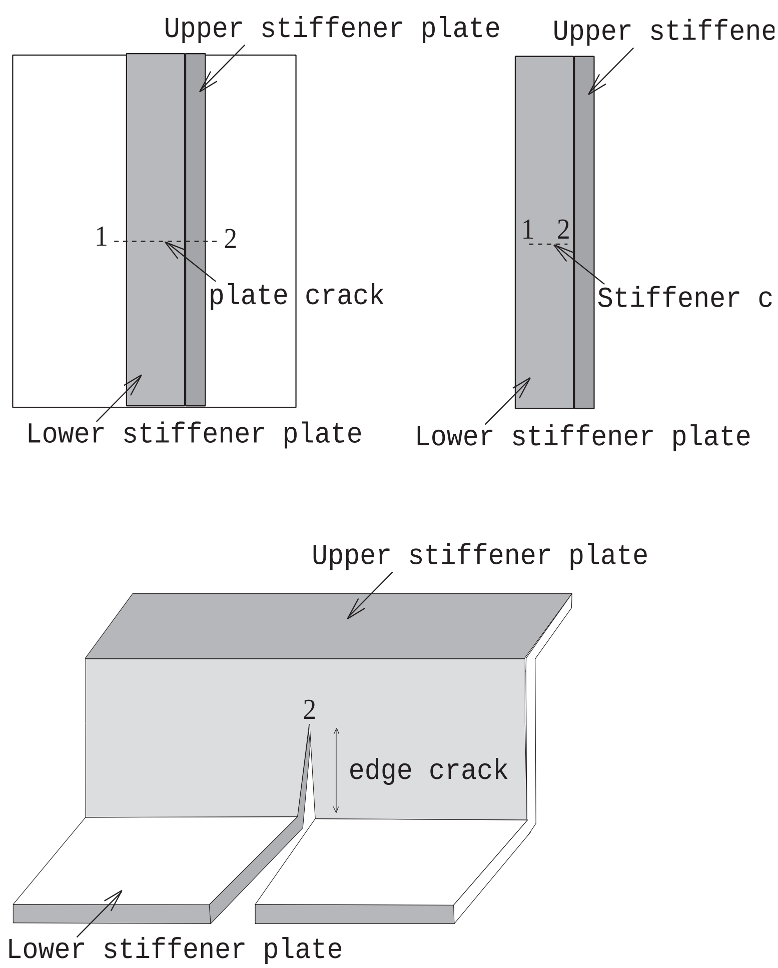

Figure 17: Stiffener riveted to plate: crack growth model

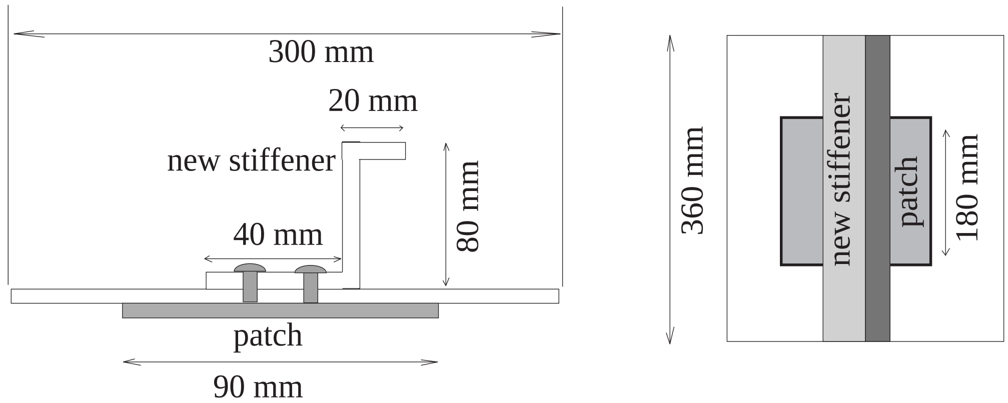

Figure 18: Patched model

$40mm \leq c \leq 160mm$ (and the lower plate of the stiffener is broken) a big raise is clear. At the end ($160mm \leq c$) the stiffener is considered completely broken as it does not carry any more load; the $K_I^{\max}$ diminish because the bending induced by the stiffener is very small compared to before and so is the K_{1b}. For both tips the behaviour is very similar, only for a small difference in K_{1b} is acknowledged caused by the asymmetric bending of the stiffener. Consider now the stiffener; at the beginning there are two tips, where the tip near the open edge has higher $K_I^{\max}$. When the crack breaks through the vertical plate, it becomes an edge crack (the other side is now open) and the $K_I^{\max}$ rises considerably. The repaired structure behaves much better, the $K_I^{\max}$ are much lower (no crack is present in the stiffener now, as it has been replaced). It has to be noticed that part of the gain is due to the new stiffener, as its contribution alone for a crack $c = 20mm$ diminish the $K_I^{\max}$ of about 13%.

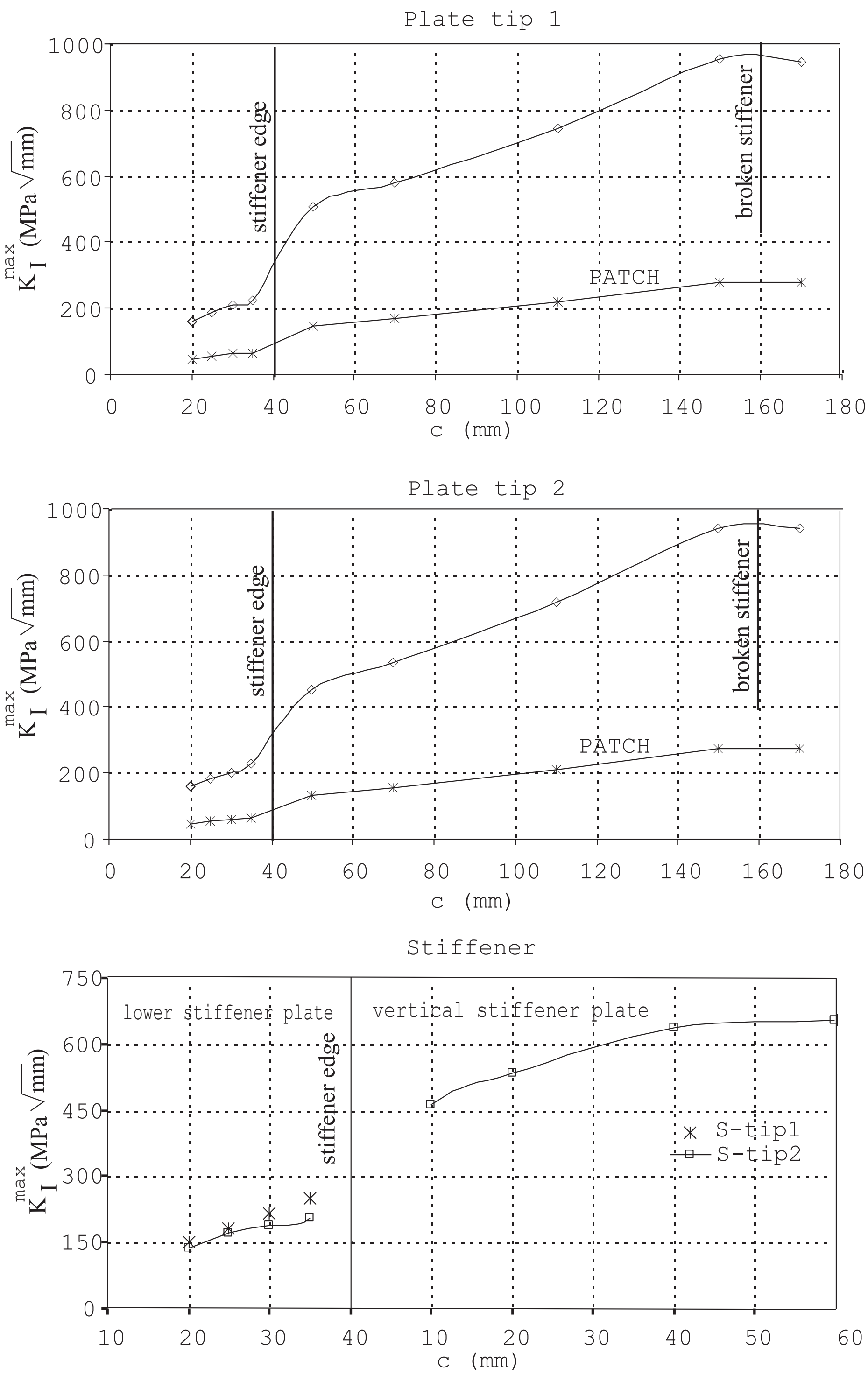

Figure 19: Stiffener riveted to plate maximum mode I stress intesity factor: against crack size

Repair of a cracked Wingbox

As last example, a wing box section is presented. In figure (20) the geometry is illustrated along with general dimensions; the section depth is the distance between two ribs (typically $640mm$). Material is taken as aluminium whose properties are Young's modulus $E = 73GPa$ and Poisson's ratio $\nu = 0.3$, for skin, spars and stiffeners. The geometry presents a three spar section, with fully stiffened skin. The thickness of the skin is taken as $2.5mm$; the rear spar is $3.5mm$ thick while the front and central spars are $4.5mm$ thick; the stiffeners at the skin and at corners are composed of plates joined through edges, of $5mm$ thickness; the stiffeners connecting the central spar to the skin are $7.5mm$ thick. Angular and skin stiffener are then riveted to the skin and the spar; the rivets arrangements are illustrated in figure (21). Typically the load is transferred to the wing box through the ribs and outer skin connections, therefore it can be considered as applied to the edges. For a general section, there is a bending moment generated by the lift, and a torsion moment, due to the eccentricity between the elastic centre of the section and the aerodynamic centre of the airfoil. The bending moment is applied via uniform traction on the lower skin and uniform compression on the upper skin; while the torsion moment is applied as shear in-plane traction along the edges. In this example the normal tension is taken as $t_x = 500N/mm$ and the in-plane shear traction as $t_y = 150N/mm$. In the position shown in figure (22), cracks of different sizes are placed and the stiffener in considered broken. The BEM model uses 148 panels, with 16 boundary elements each, 4 on each side. Stiffeners are considered as solid pieces and are joined through the edges, while connections to spars and skin is modelled with rivets. The crack is modeled with 16 discontinuous boundary elements. Then a rectangular patch of dimension ($300mm \times 90mm$) and of thickness $2.5mm$ is attached on the crack. The patch is made of aluminium and is modelled with 16 boundary elements, and 79 bonding points are regularly placed in the bonded area. The broken stiffener is replaced with new one.

In figure (23) $K_I^{\max}$ and $K_{II}^{\max}$ are plotted against crack size, for both tips, with and without patch. The applied torsion cause mode II opening, the crack growth angle has been evaluated as about 60^o for both tips; the SIFs are high, the crack will grow quickly. Again the recovery of the structure due to the repair is clear. It has to be noticed the tip 2 SIFs are higher because of the bending induced by the asymmetric stiffeners.

Colour contours of U_y displacements are shown in figures (24)-(25); where it can be seen the effects of the crack. It does not effect the entire structure, but the local effects are quite large. Contact is not modelled, therefore some interpenetration can be seen.

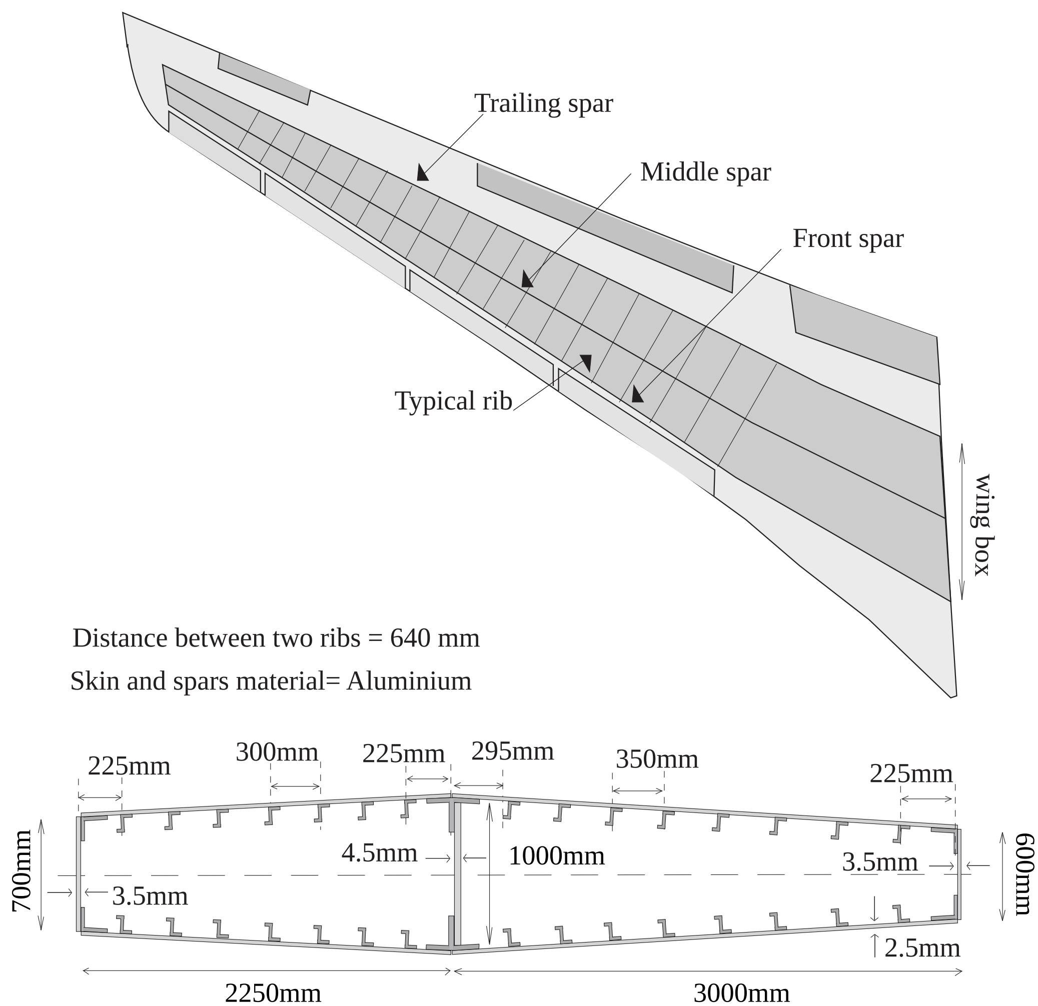

Figure 20: Wing box: geometry

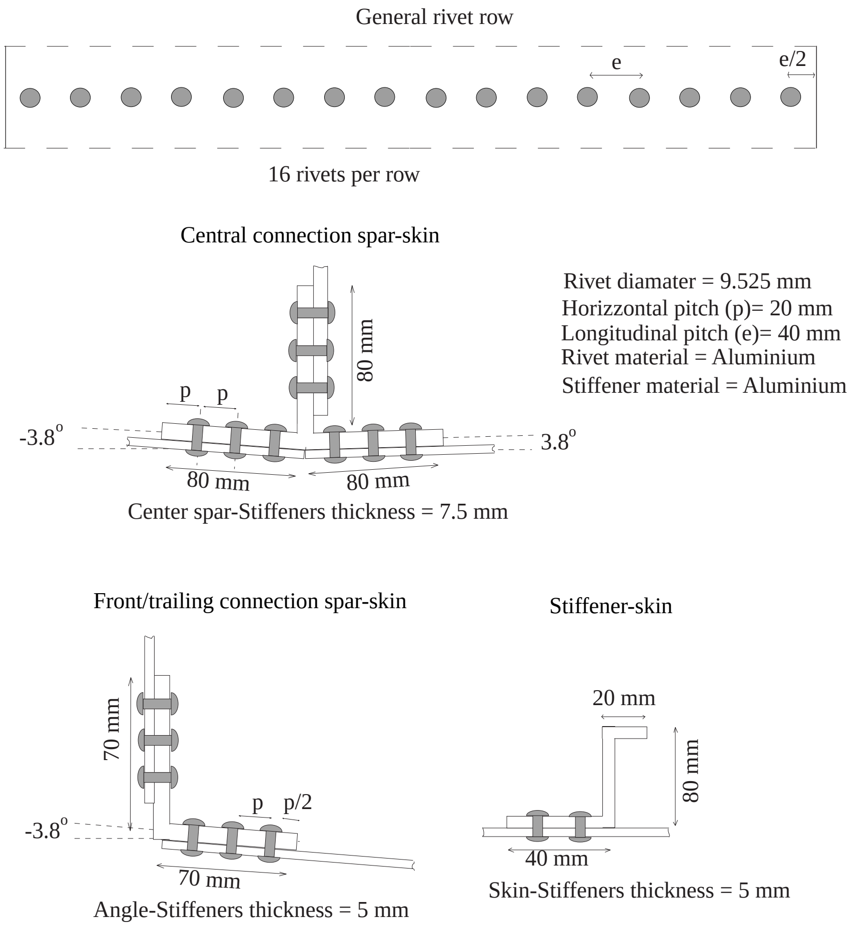

Figure 21: Wing box: rivet arrangements

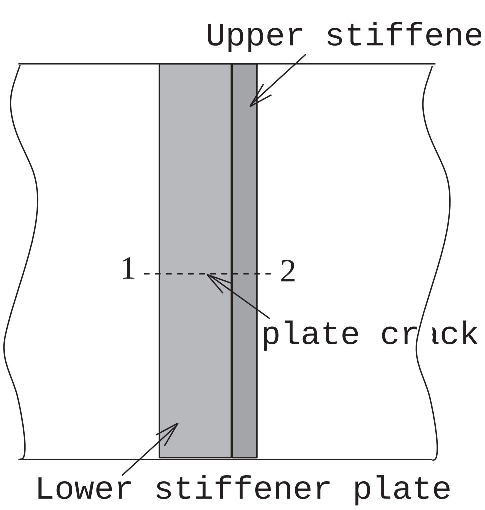

Figure 22: Wing box: crack geometry

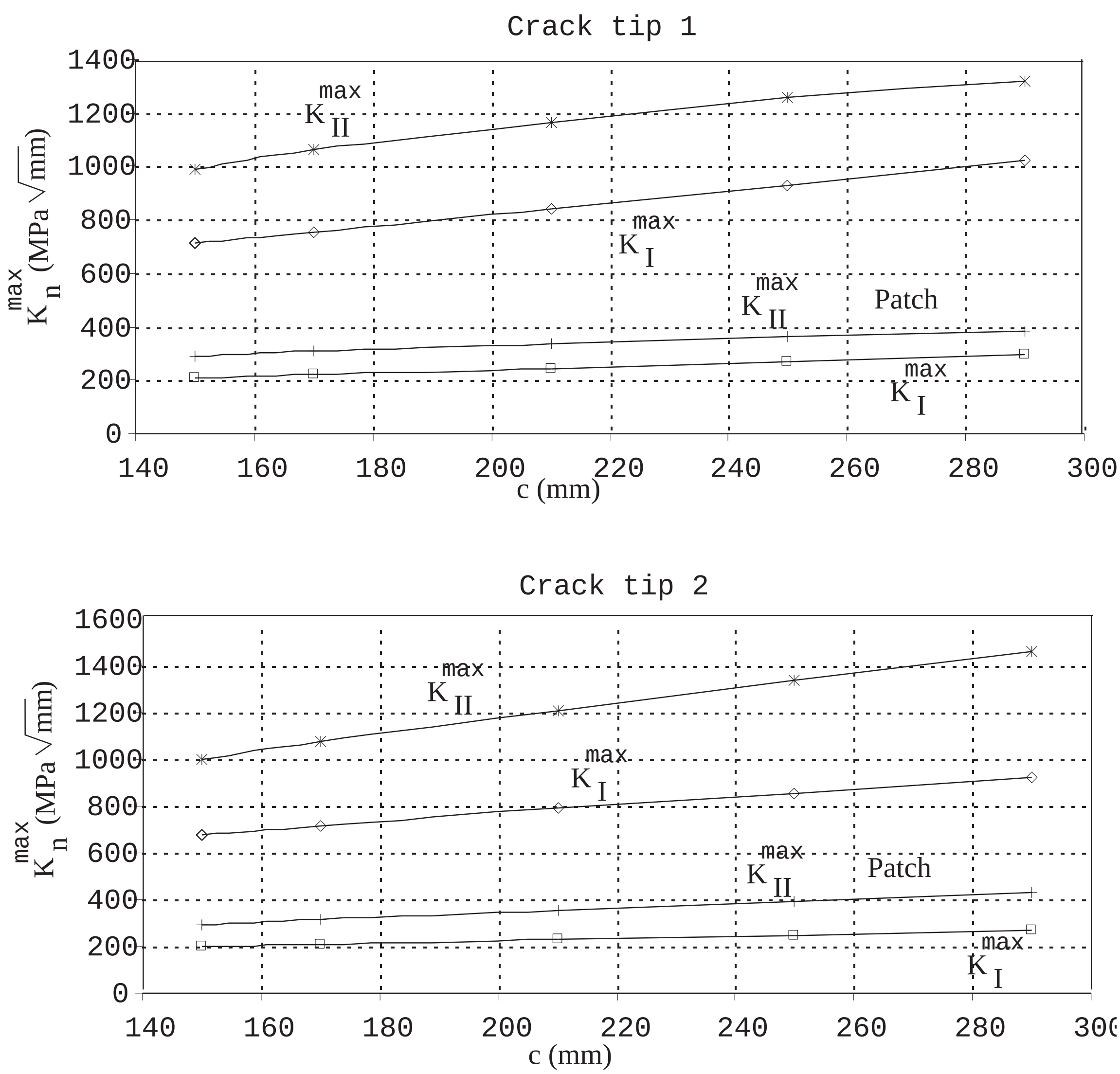

Figure 23: Wing box: SIFs against crack size

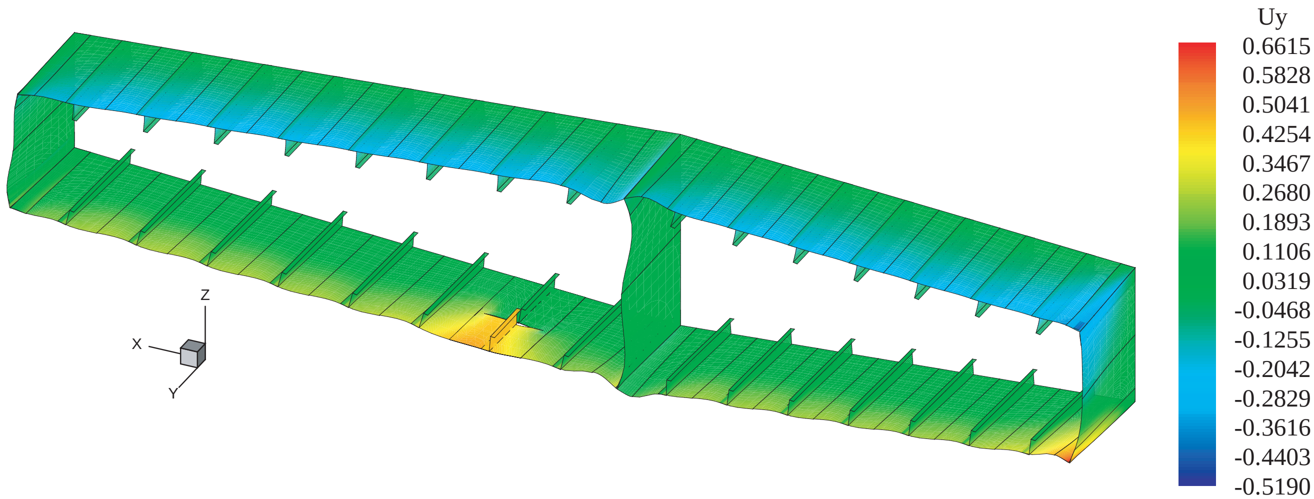

Figure 24: Wing box: vertical disaplacement colour contours

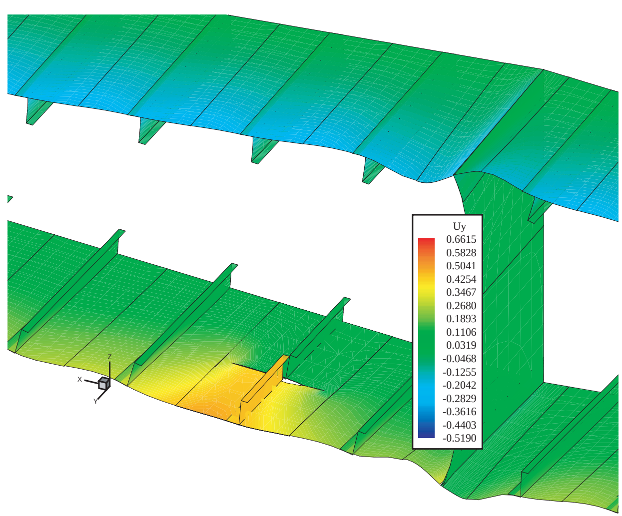

Figure 25: Wing box: vertical displacement colour contours close-up

Conclusions

In this paper a feasibility study for applying the boundary element method to the analysis of stiffened panels repaired with patches was presented. In order to achieve such feature, several formulations were combined together to analyse the model. The multi-region formulation was used to simulate the stiffeners, which were modelled as an assembly. A boundary element formulation for rivets was employed to connect the stiffeners to the sheets; while the dual boundary element method was implemented to simulate the presence of cracks. The patches were attached either with rivets or adhesively bonded. The latter was modelled by means of a dedicated boundary element formulation for adhesive bonding. The dual boundary element method was applied to model the cracks, and the COD method and the J-integral were implemented to extract the stress intensity factors. Examples were presented to validate the proposed formulations, and results were found satisfactory. A study of crack running through a stiffened panel was presented as well, then the repaired geometry was examined to investigate the relief due to the repair. At the end a wing box section was analysed to show the possible applications of the proposed method. The combination of the formulations are found to provide an effective numerical tool, capable of performing the analysis of complex structures.

References

[1] Actis, R.L, Szabò, B.A, *Analysis of Bonded and Fastened Repairs by the p-Version of the Finite-Element Method,* Computer and Mathematics with Applications, vol. 46, pp 1-14, (2003)

[2] Albuquerque,EL, Sollero,P., Venturini,W.S. and Aliabadi,MH; Boundary element analysis of anisotropic Kirchhoff plates; International journal of solids and structures 43 (14), 4029-4046 (2006)

[3] Aliabadi,MH., Plate bending Analysis with Boundary Elements, Computational Mechanics Publications, Southampton, (1998).

[4] Aliabadi, M.H., *The Boundary Element Method, vol II: application to solids and structures*, Winchester, Wiley (2001)

[5] Aliabadi, M.H., *A new generation of boundary element methods in fracture mechanics,* International Journal of Fracture, vol. 86, pp 91-125, (1997)

[6] Aliabadi, M.H., *Boundary element formulations in fracture mechanics,* Applied Mechanics Review, vol. 50, pp 83-96, (1997)

[7] Baiz, P.M. and Aliabadi, M.H., Local buckling of thin-walled structures by the boundary element method, Engineering Analysis with Boundary Elements, v 33, n 3, p 302-313, (2009)

[8] Baker, A.A., Jones, R., *Bonded Repair of Aircraft Structures,* Martinus Nijhoff Publishers, Dordrecht (1988)

[9] Balas,J., Sladek,J and Sladek,K The boundary integral equation method for plates resting on a two-parameter foundation, ZAMM, vol 64, pp137-146 (1984).

[10] Barcellos,CA and Silva,LHM., A boundary element formulation for the Mindlin's plate model, in Boundary Element Technology, Computational Mechanics Publications, Southampton, pp123-130 (1989).

[11] Benedetti,I, Aliabadi,MH A three-dimensional cohesive-frictional grain-boundary polycrstaline materials, Computer Methods in Applied Mechnaics and Engineering, v 265, 36-62 (2013)

[12] Bezine,G Boundary integral formulation for plate flexture with arbitrary boundary conditions, Mech. Research Communications, vol 5(4), pp197-206 (1978).

[13] Di Pisa, C. ; Aliabadi, M.H., An efficient BEM formulation for analysis of bond-line cracks in thin walled aircraft structure; International Journal of Fracture, v 179, n 1-2, pp 129-145, (2013)

[14] Di Pisa, C. ; Aliabadi, M.H., Fatigue crack growth analysis of assembled plate structures with dual boundary element method; Engineering Fracture Mechanics, v 98, pp 200-13, (2013)

[15] Di Pisa, C. ; Aliabadi, M.H. and Yong,A., Dual boundary method for assembled plate structures undergoing large deflection; International Journal for Numerical Methods in Engineering, v 89, n 13, pp 1720-38, 30 (2012).

[16] Dourakopoulos, J.A.; Sapountzakis, E.J.Nonlinear dynamic analysis of plates stiffened by parallel beams with deformable connection, Advances In Civil Engineering, p 942763 (22 pp.), (2014)

[17] Dirgantara, T. and Aliabadi, M. H., *Boundary element method analysis of assembled plate-structure,* Communications in numerical methods in engineering, vol.17, pp. 749-760, (2001)

[18] T Dirgantara, MH Aliabadi; Crack growth analysis of plates loaded by bending and tension using dual boundary element method; International journal of fracture 105 (1), 27-47

[19] Dirgantara, T. and Aliabadi, M. H., *Stress Intensity Factors for cracks in thin plates,* Engineering Fracture Mechanics, vol.69, pp. 1465-1486, (2002)

[20] Dirgantara, T. and Aliabadi, M. H., *Dual boundary element formulation for fracture mechanics analysis of shear deformable shells,*International Journal of Solids and Structures, vol. 38, pp.7769-7800, (2001)

[21] Fedelinski,P., Aliabadi,MH. and Rooke,DP., The Laplace transform DBEM for mixed-mode dynamic crack analysis; Computers & structures 59 (6), 1021-1031, (1996).

[22] Forbes,DJ and Robinson,AR Numerical analysis of elastic plates and shallow shells by an integral equation method, structural research series report no 345, university of Illinois, Urbana, USA (1969).

[23] Fernandes, Gabriela RA., BEM formulation for linear bending analysis of plates reinforced by beams considering different materials Engineering Analysis with Boundary Elements, v 33, n 8-9, p 1132-1140, (2009)

[24] Goland, M. and Reissner, E., *The Stresses in Cemented Joints,* ASME, A-17 A-27, March (1944)

[25] Hartmann,F and Zormantel,R, The direct boundary element method for plate bending, International Journal for Numerical Methods in Engineering, vol 23, pp2049-2069 (1986).

[26] Huang,X, Aliabadi,MH and Sharif Khodaei, Z Fatigue crack growth reliability analysis by stochastic boundary element method, CMES: Computer Modeling in Engneering & Sceinces, v 102, 291-330 (2014).

[27] Hwu, Chyanbin, Boundary element formulation for the coupled stretching-bending analysis of thin laminated plates, Engineering Analysis with Boundary Elements, v 36, n 6, p 1027-1039, (2012)

[28] Jaswon,MA, Maiti,M and Symm,GT., Numerical biharmonic analysis and some applications, International Journal of Solids and Structures, vil 3, 309-332 (1967).

[29] Kamiya,N and Sawaki,Y An integral equation approach to finite deflection of elastic plates, international journal of Non-linear Mechanics, vol 17, 187-194 (1988).

[30] Karam,VJ and Telles,JCF On boundary elements for Reissner's plate theory, Engineering Analysis, vol 5, pp21-27 (1988).

[31] Katsikadelis,JT and Nerantzaki,MS, The boundary element method for non-linear problems, Engineering Analysis with Boundary Elements, vol 23, pp365-373 (1999).

[32] Katsikadelis, J.T. and Babouskos, N.G.; Stiffness and buckling optimization of thin plates with BEM; Archive of Applied Mechanics, v 82, n 10-11, p 1403-1422, (2012).

[33] Kirchhoff,G., Uber das gleichgewicht und die bewegung einer elastischen scheibe, J Rein Angew Math, vol 40, pp51-88 (1850).

[34] Lei,XY, Haung,MK and Wang,XX., Geometrically nonlinear analysis of a Reissner type plate by the boundary element method, Computers and Structures, vol 37, pp911-916 (1990).

[35] Lucas, F.M, *et al., Multiple-site damage in riveted lap-joints: experimental simulation and finite element prediction,* International Journal of Fatigue, vol. 22, pp 319-338, (2000)

[36] Mackerle, J., *Finite element analysis of fastening and joining: A bibliography (1990-2002),* International Journal of Pressure Vessels and Piping, vol. 80, pp 253-273, (2003)

[37] Maleki, S. and Tahani, M., Non-linear analysis of moderately thick laminated plates and shell panels under thermo-mechanical loading, Zeitschrift fur Angewandte Mathematik und Mechanik, v 92, n 8, p 652-67 (2012)

[38] Mi,Y and Aliabadi,MH, Dual boundary element method for three-dimensional fracture mechanics analysis Y Mi, MH Aliabadi Engineering Analysis with Boundary Elements 10 (2), 161-171(1992).

[39] Müller, R.P.G., *An Experimental and Analytical Investigation of the Fatigue Behaviour of Fuselage Riveted Lap Joints,* Delft University of Technology, Delft, Netherlands (1995)

[40] Murakami, Y. (Ed.), *Stress Intensity Factors Handbook,* Oxford, Pergamon Press (1987)

[41] Panzeca, T., Milana, V. and Salerno, M.; A symmetric Galerkin BEM for plate bending analysis Source: European Journal of Mechanics, A/Solids, v 28, n 1, p 62-74, (2009).

[42] Pavia,JB and Aliabadi,MH Boundary element analysis of zoned plates in bending, Computational Mechanics, vol 25, pp560-566 (2000).

[43] Poe, C.C., *The effect of riveted and uniformly spaced stringers on the stress intensity factors of a cracked sheet.* MSc thesis, Virginia Polytechnic Institute, (1969)

[44] Provatidis, C.G. and Angelidis, D.I., Performance of Coons' macroelements in plate bending analysiInternational Journal of Computational Methods in Engineering Science and Mechanics, v 15, n 2, p 110-125, (2014)

[45] Purbolaksono, J.; Aliabadi, M.H. Buckling analysis of shear deformable plates by boundary element method International Journal for Numerical Methods in Engineering, v 62, n 4, p 537-563, (2005).

[46] Purbolaksono, J. and Aliabadi, M.H. Source: Dual boundary element method for instability analysis of cracked plates, Computer Modeling in Engineering & Sciences, v 8, n 1, p 73-90, (2005)

[47] Portela, A. and Aliabadi, M.H., *The Dual Boundary Element Method: Effective Implementation For Crack Problems,* International Journal for Numerical Methods in Engineering, vol.33, pp. 1269-1287, (1992)

[48] Rashed,YF, Aliabadi,MH and Brebbia,CA., The boundary element method for thick plates on a Winkler foundation, International Journal of Numerical Methods in Engineering, vol 41, pp1435-1462 (1998).

[49] Ratwani, MN., *Analysis of cracked adhesively bonded laminate structures.* AIAA Journal, vol. 17, pp. 988-94, (1979)

[50] Reissner,E., On bending of elastic plates, Quarterly Journal of Applied Mathematics, vol 5, pp55-68 (1947).

[51] Rigby, R.H. and Aliabadi, M.H., *Mixed-mode J-integral method for analysis of 3D fracture problems using BEM,* Engineering Analysis with Boundary Elements, vol.11, pp.239-256, (1993)

[52] Salgado, N. K. and Aliabadi, M. H., *The application of the dual boundary element method to the analysis of cracked stiffened panels*, Engineering Fracture Mechanics, vol. 54, pp. 91-105, (1996)

[53] Salgado, N. K. and Aliabadi, M. H., *Boundary element analysis of cracked stiffened sheets, reinforced by adhesively bonded patches*, International Journal for Numerical Methods in Engineering, vol. 42, pp. 195-217, (1998)

[54] Salgado, N.K., Aliabadi, M.H., *The Analysis of Riveted Repairs and Lap Joints,* Fatigue and Fracture of Engineering Materials and Structures, vol 20 (4), pp. 583-93, (1996).

[55] Sapountzakis, E.J., and Dikaros, I.C.; Large deflection analysis of plates stiffened by parallel beams; Engineering Structures, v 35, p 254-271, (2012).

[56] Sfantos,GK and Aliabadi,MH A boundary cohesive grain element formulation for modelling intergranular microfracture in polycrystalline brittle materials, International Journal of Numerical Methods in Engineering, v 69, 1590-1626 (2007).

[57] Sharif Khodaei,Z, Ghajari,M and Aliabadi,MH Determination of impact location on composite stiffened panels, Smart Materials and Structures, v 21(10), 105026 (14 pages), (2012).

[58] Shi,G and Bezine,G A general boundary integral formulation for the anisotropic plate bending problems, Journal of Composite Materials, vol 22, 694-716 (1988).

[59] Stern,M., A general boundary integral formulation for plate bending problems, International Journal of Solids and Structures, vol 15, pp769-782 (1979).

[60] Syngellakis,S and Elzein,A., Plate buckling loads by the boundary element method, International Journal for Numerical Methods in Engineering, vol 37, pp1736-1778 (1994).

[61] Swift, T., *Development of the fail-safe design feature on DC-10,* ASMT_STP 486, pp.164-214, (1971)

[62] Tanaka,M and Miyazaki,K., A direct BEM for elastic plate-structure subjected to arbitrary loadings, in Boundary Elements VII, Springer Verlag, Berlin, 4-3, 4-16 (1985).

[63] Tanaka, M; Matsumoto, T and Yamamura, H.; Application of BEM with extended Kalman filter to parameter identification of an elastic plate under dynamic loading Engineering Analysis with Boundary Elements, v 28, n 3, p 213-219, (2004)

[64] Telles,JCF and Karam,VJ., Nonlinear material analysis of Reissner's plates, in Plate bending with boundary elements, Computational Mechanics Publications, Southampton, 127-164 (1998).

[65] Tottenham,H., The boundary element method for plates and shells, in Developments in Boundary Element Methods -I, Applied Science, London, pp173-205 (1979).

[66] Useche, J. and Albuquerque, E.L. Dynamic analysis of shear deformable plates using the dual reciprocity method; Engineering Analysis with Boundary Elements, v 36, n 5, p 627-632, (2012)

[67] Vander Weeen, F. *Application of the boundary integral equation method to Reissner's plate model,* International Journal of for Numerical Methods in Engineering, vol. 18, pp. 1-10, (1982)

[68] Fernandes, G.R. and Venturini,W.S.; Stiffened plate bending analysis by the boundary element method; Computational Mechanics, v 28, n 3-4 SPEC., p 275-281, (2002).

[69] Young, A., Cartwright, D.J., Rooke, D.P., *The boundary element method for analyzing repairs patches of cracked finite sheets,* Aeronautical Journal,vol.92 (17), pp. 416-421, (1988)

[70] Young, A., Rooke, D.P., Cartwright, D.J., *Analysis of patched and stiffened cracked panels using the boundary element method,* International Journal of Solids and Structures, vol.29 (17), pp. 2201-2216, (1992)

[71] Wen, P.H, Aliabadi, M.H and Young, A., *Boundary element analysis of flat cracked panels with adhesively bonded patches,* Engineering Fracture Mechanics, vol.69, pp. 2129-2146 (2002)

[72] Westphal,T,Jr. and Barcellos,CA., Application of the boundary element method to Reissner's and Mindlin's plate model, in Boundary Elements XII, Computational Mechanics Publication, Southampton, vol 1, pp467-477 (1990).

[73] Wen, P.H. and Aliabadi, M.H.; Young, A.; A boundary element method for dynamic plate bending problems; International Journal of Solids and Structures, v 37, n 37, p 5177-88, (2000).

[74] Wen, P. H., Aliabadi, M. H. and Young, A., *Fracture mechanics analysis of curved stiffened panels using BEM,* International Journal of Solids and Structures*,* vol 40, pp. 219-236, (2003)

[75] Widagdo, D., Aliabadi, M.H., *Boundary element analysis of cracked panels repaired by mechanically fastened composite patches,* Engineering Analysis with Boundary Elements, vol.25, pp. 339-345, (2001)